DETERMINATION OF THE STATIC PERFORMANCE OF FINITE ELASTO-HYDRODYNAMIC JOURNAL BEARINGS LUBRICATED BY MAGNETIC FLUIDS WITH COUPLE STRESSES

DANIEL KARIUKI KIHUGA

MASTER OF SCIENCE

(Applied Mathematics)

JOMO KENYATTA UNIVERSITY OF AGRICULTURE AND TECHNOLOGY

2014

2013

MSC.

KIHUGA D. K.

Determination of the static performance of finite elasto-hydrodynamic

journal bearings lubricated by magnetic fluids with couple stresses

DANIEL KARIUKI KIHUGA

A thesis submitted in partial fulfillment for the degree of Master of Science

in Applied Mathematics in Jomo Kenyatta University of Agriculture and

Technology

2014

DECLARATION

This thesis is my original work and has not been presented for a degree in any other university.

Signature: _____   Date: _____

       Daniel Kariuki Kihuga

This thesis has been submitted for examination with our approval as university supervisors

Signature: _____   Date: _____

       Prof. Mathew Kinyanjui

       J.K.U.A.T, Kenya

Signature: _____   Date: _____

       Dr. Mark Mwiti Kimathi

       TUK, Kenya

DEDICATION

This piece of work is dedicated to my loving mum Lucy Kihuga, my dad Samuel Kihuga, and my siblings Mercy, Stephen, James and Grace. To mum and dad: Thank you for your love, care, endurance, inspiration, financial support and mostly for your prayers. To you my siblings, Thank you for lifting me up when I was down and for encouragement.

ACKNOWLEDGEMENTS

TABLE OF CONTENTS

LIST OF FIGURES

LIST OF APPENDICES

LIST OF ABBREVIATIONS/ACRONYMS

RPM   Rotations per Minute

EHL   Elasto hydrodynamic Lubrication

MHD   Magneto hydrodynamic

THL   Thermo hydrodynamic Lubrication

CFD   Computational fluid dynamics

LIST OF NOMENCLATURES

Romans Symbol	Quantity
C	Bearing clearance, (m)
e	Eccentricity of the journal center, (m)
ε	Eccentricity ratio $\left(\varepsilon = e/C\right)$
F_m	Unit volume value of the induced magnetic force, *Tesla*
F_{mx}	Magnetic force in x direction (circumferential direction)
F_{mz}	Magnetic force in z direction (axial direction)
M_g	Magnetization of the magnetic material, Wbm^{-2}
M_{gs}	Saturation value of magnetization
$\mathcal{B}$	Magnetic field density vector, *Tesla*
h	Lubricant film thickness, (m)
H	Non-dimensional film thickness $\left(H = h/C\right)$
u_i	Fluid velocity vector in x, y and z directions
u, v, w	Components of velocity vector $\vec{q}$ $\left(ms^{-1}\right)$
u^*, v^*, w^*	Dimensionless velocity components
x, y, z	Cartesian coordinates
θ	Angular coordinate $\left(x/R\right)$
R	Bearing or journal radius
Z	Non-dimensional axial distance $\left(Z = z/L_b\right)$

x

X_m	Susceptibility of ferro-fluid
h_{max}	Maximum film thickness, (m)
h_{min}	Minimum film thickness, (m)
T	Lubricant temperature
T_w	Lubricant inlet temperature (at the bearing)
T_∞	Lubricant temperature (at the journal)
T^*	Non-dimensional temperature
C_p	Specific heat
h_m	Magnetic field intensity, Wbm^{-2}
h_{m0}	Characteristic value of magnetic field intensity
H_m	Non-dimensional magnetic field intensity $\left(H_m = h_m/h_{m0}\right)$
P	Lubricant pressure, N/m^2
P^*	Non-dimensional pressure
α	Magnetic force coefficient
λ_0	Permeability of free space or air $\lambda_0 = 4\pi.10^{-7} \, AT/m$
ρ	Fluid density, Kg/m^3
μ	Fluid viscosity, pa-s
μ^*	Non-dimensional viscosity
l	Couple stress parameter *Tesla*
L	Non-dimensional couple stress parameter $\left(L = l/C\right)$
m	Number of mesh points in axial direction

n	Number of mesh points in circumferential direction
ω	Angular speed, rad/s
ϕ	Attitude angle,
η	Material constant responsible for the couple stress property
$\vec{\nabla}$	Gradient operator $i\dfrac{\partial}{\partial x}+j\dfrac{\partial}{\partial y}+k\dfrac{\partial}{\partial z}$
$\vec{F}$	Body forces vector in x, y and z directions
υ	Kinematic viscosity, $m^2 s^{-1}$

ABSTRACT

This study concerns the theoretical determination of static performance of finite elasto-hydrodynamic journal bearings lubricated by ferro-fluids with couple stresses. The Reynolds equation that takes into account magneto elasto-hydrodynamics is derived by use of continuity and momentum equations. The equation has been integrated locally across the film thickness and an equation for the pressure gradient obtained as a function of film thickness and total mass flow rate of lubricant, now the modified Reynolds equation. The modified Reynolds equation obtained is solved simultaneously with the energy equation numerically by the finite difference technique since they are highly non-linear. The pressure and temperature profiles are obtained. The numerical scheme used is implemented in MATLAB software version 7.14.0.739, so as to obtain the approximate solutions where these solutions are represented in tables and graphs. Based on the micro-continuum theory, and by taking into account the couple stresses due to the microstructure additives, the effects of couple stresses on the performance of a finite elasto-hydrodynamic journal bearings were studied. The results were obtained by varying various flow parameters, notably couple stress parameter, magnetic coefficient and eccentricity ratio. From the results it was found that the magnetic lubrication gives higher pressure distribution. The results have also shown that lubricants with couple stresses compared with Newtonian lubricants increase the pressure especially at high eccentricity ratios. Thus it can be concluded that magnetic fluids lubricants with couple stresses are better than Newtonian fluids. The results provide engineers with useful information to design machine elements and bearing systems with a higher life expectancy and efficiency.

CHAPTER ONE.

INTRODUCTION

1.0 Background of the Study

In centuries, the study and investigation of the performance of the hydrodynamic journal bearing under different modes of loading have been done. This type of bearings is one of the most commonly used in a wide variety of machines. A bearing is a system of machine elements whose function is to support an applied load by reducing friction between the relatively moving surfaces. When designing such lubricating system, the heat, load and flow rate required for a bearing must be known to properly size the lubricating oil pumps, coolers among other bearing machines. Bearing type and size are based on rotor weight, rotor rotations per minute (RPM), and lubricant characteristics Govindaraj *et al* (2012).

The characteristics of hydrodynamic journal bearing have been the subject of many researches. Some being directed to the bearing geometry design and others devoted to the study of the lubricant properties. The introduction of lubricants that had additional characteristics, compared with conventional lubricants, led to an improvement of the bearing performance. These non-conventional lubricants are referred to as Ferro-fluid lubricants or magnetic fluid lubricants.

The resent solutions that have encouraged the study of the lubricant properties have been devised with other parameter being considered in predicting the journal bearing behavior, such as load carrying capacity, type of lubricant flow region (laminar or turbulent flow), type of lubricant (Newtonian or non-Newtonian), inertia and acceleration effects, and magnetic effect in the case of using Ferro-fluid (Osman, 2002). Thermo-Elasto-hydrodynamic analysis of a diaphragm journal bearing have also been done with the view of optimizing bearing performance, predicting

and comparing the bearing characteristics with the thermo-hydrodynamic models (Norman, 1995)

Most of these investigations considered only the isothermal cases and neglected viscosity variation with change of temperature. With time, the thermal aspects have been investigated together with the journal bearing behavior lubricated by magnetic fluids with couple stress Abdo *et al* (2009). The latter again neglected the effect of joules heating on the performance of the journal bearing. Practically, increasing in load capacity leads to increasing the friction force, shear stress and consequently increasing the lubricant temperature. Although many aspects of bearing performance are solved, there are still needs for further studies of the thermal effects on the bearing performance and characteristics.

Lubrication

Wear and tear occurs when two plates in contact move with relative velocity causing high friction between them. To reduce this friction, a thin layer of fluid with high viscosity is applied between them. This arrangement is referred to as bearing and the fluid applied between the plates is known as a lubricant. Lubrication is therefore the process employed to reduce wear and tear of one or both surfaces of the plates in close proximity and moving with relative velocity over each other. This is achieved by interposing lubricant between their surfaces to help carry the load supported by the bearing. The three types of lubrication regimes are boundary lubrication, elasto-hydrodynamic lubrication (mixed film lubrication) and hydrodynamic lubrication. Boundary lubrication is where by the surfaces are in contact to each other. Elasto-hydrodynamic lubrication (EHL) is a form of fluid film lubrication where the elastic deformation of the lubricated surfaces cannot be neglected leading to the surfaces being in contact at some points. On the contrary, this effect might even be dominant leading to the boundary lubrication case. However, the EHL theory is applicable for lower loads and less rigid structures such as journal

bearing. In the case of the hydrodynamic lubrication (full fluid film lubrication) the surfaces are separated completely by the fluid film, so the lubricating fluid carries the entire load exerted on the two surfaces. This kind of fluid film lubrication is usually associated with highly stressed machine elements, such as rolling element bearings and gears. In this work, we shall assume an elasto-hydrodynamic case in a journal bearing.

Ferro-fluid

In this study a non-conventional lubricant called ferro-fluid lubricant or magnetic fluid lubricant is used. A Ferro-fluid is composed of three basic components namely; ferromagnetic particles, a base fluid or carrier fluid and a coating on each particle as shown in figure (1.1) Raj and Boulton (1987). Examples of the base fluid may include a hydrocarbon base, an ester base, a diester base or even water base are among the base fluids important for lubrication.

The ferromagnetic particles in the base fluid are small in size so as to prevent agglomeration by gravitational forces thus a colloidal suspension of these particles can be obtained. The most usual ferromagnetic minerals are magnetite (Fe_3O_4), iron, cobalt, nickel and their alloys. Every ferromagnetic particle is coated with a thin layer (1-2 nm thick) of polymer molecules. These monomolecular surfactants act as a dispersing agent. They keep the magnetic particles far enough apart that the attractions between the particles, due to Vander Waals force or the magnetic force does not cause agglomeration of these particles since this could affect the performance of the lubricant.

3
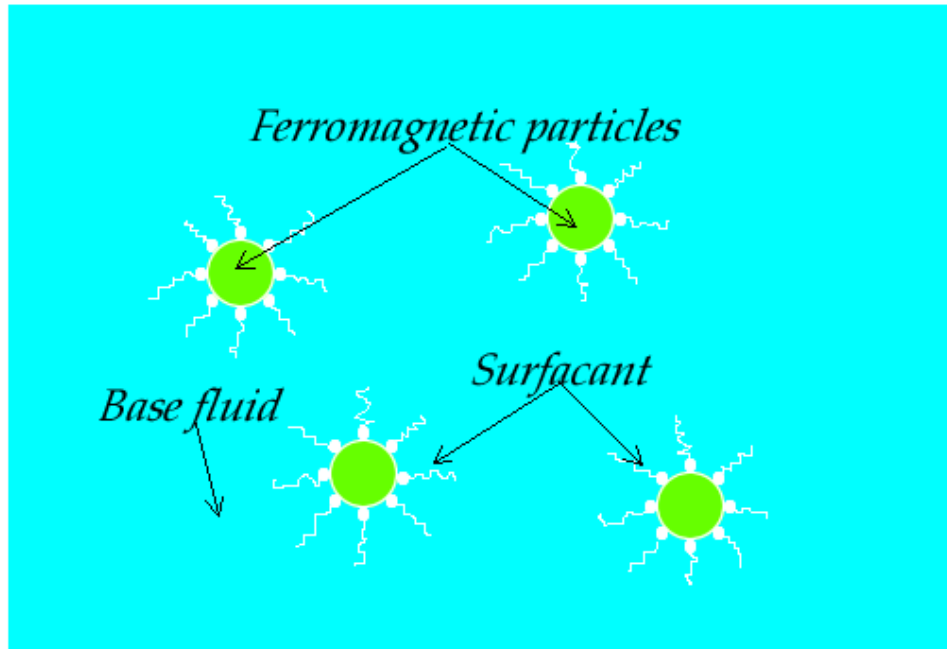
Figure 1.1: Components of a ferro-fluid

Therefore, the ferro-fluids are very stable. Many properties of the ferro-fluid are similar to those of the base fluid. The concentration of the magnetic particles is low and thus they do not affect the density, vapor pressure, pour point, or chemical properties of the liquid. There is an increase of the ferro-fluid viscosity compared with the viscosity of its base fluid. The electrical properties of ferro-fluids are also similar to those of base fluids. This implies that the magnetic fluids are non-conductive except where there is a metallic base fluid. The ferro-fluid acts like pure iron in that it does not have any magnetic activity in the absence of the magnetic field. It gets magnetized in the presence of the magnetic field. When a magnetic field is applied to the Ferro-fluid, each particle experiences a force that fully depends on the magnetization of the magnetic material of the particles and on the strength of the applied field.

Ferro-fluids lubrication applies the Navier-Stokes equation where it is modified by adding a term to take into account the effect of its magnetic property. It is therefore true that in the absence of magnetic field, the Ferro-fluid acts like other liquids, but in the presence of magnetic field, it is affected by an additional magnetic force.

In decades, researches have indicated that these ferro-lubricants are magnetically stable and function well as lubricant (Moskowitz, 1975). Therefore, these ferro-lubricants can be controlled remotely by a magnetic field. They can be positioned exactly where wear would be expected to take place. This ability of positioning the lubricant externally is valuable in clean-environment applications, because the lubricant does not contaminate the environment.

Rolling bearings in industries are one successful application of magnetic oil lubrication. It is also possible to make a rolling bearing without sealing or to make a combination that includes a magnetic-oil-lubricated bearing and a magnetic fluid seal. Hydrodynamic slider bearing among other bearings can also be lubricated with magnetic oil. Some of the greatest advantages of the magnetic-oil-lubricated bearings are a long life, low friction and reduced noise. Bearings lubricated with magnetic oils have been used in fast-rotational textile industry spindles that must stay clean. Other possible applications are robots working in clean environments and computer disk drives.

Journal Bearing Mechanism

Journal bearing is a subset of bearings used to support rotating shafts that use the principle of hydrodynamic lubrication. The journal bearing is made up of four main parts as shown in the figure 1.2. These parts include; the shaft, removable shell halves, the bearing shell which supports the shell halves and the oil reservoir responsible for the bearing action.
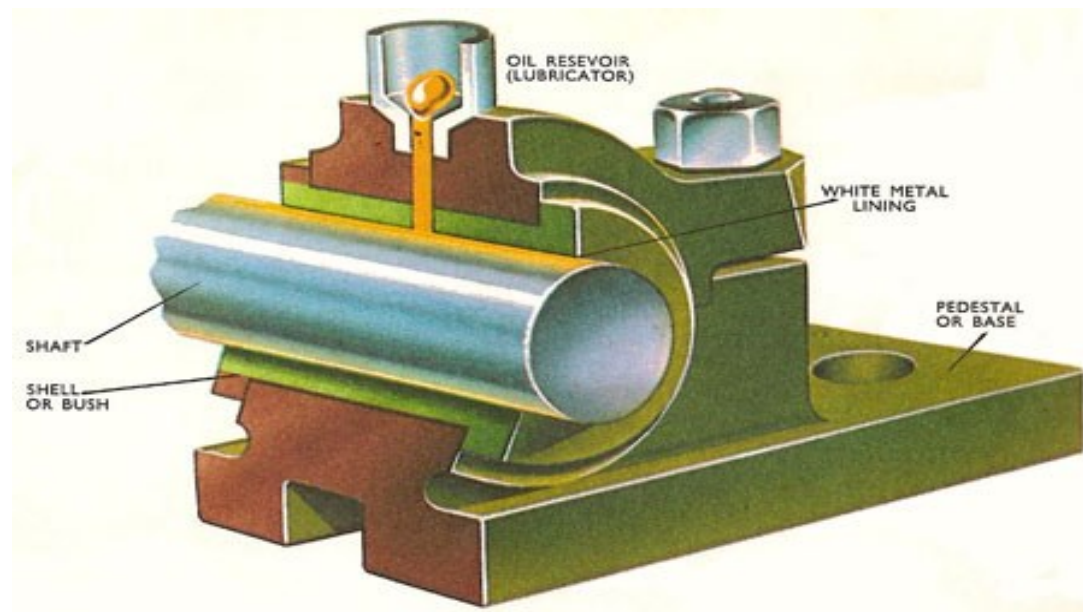
Figure 1.2: Parts of a journal bearing.

As opposed to the anti-friction bearing that operates using rolling components inside the bearing (i.e. balls, rollers), journal bearing operate by using a self-generated hydrodynamic lubricant film pressure to support the shaft while preventing the shaft from being in contact with the bearing surface. A journal bearing that uses hydrodynamic lubrication has an infinite expected life unless there is a loss of the lubricant film due to lack of lubrication or excessive force as opposed to the anti-friction bearings which have predictable life. A journal bearing simply performs where by the shaft or "journal" rotates in the bearing with a layer of lubricant separating the two plates through fluid dynamic effects. Since the bearing surfaces are moving with relative velocity, lubricant will be drawn into the gap between them and forced to squirt out the sides of the bearing while the gap is converging. As the lubricant is drawn into the converging wedge by relative motion, the pressure increases and the lubricant is forced out through the sides of the bearing since the lubricant is relatively incompressible. The self-generated pressure is what supports the load imposed by the shaft (Abdo, 2009). If the lubricant film is diverging i.e. getting

6

thicker, the pressure tends to decrease so that it can balance the load. In our study we shall examine a journal bearing as the one in the figure 1.3

Stationary Rigid Bushing

h_{max}

Θ X

y

W

O_B

e

O_J

ω

Rotating Rigid Journal

Radius R

h_{min}

L
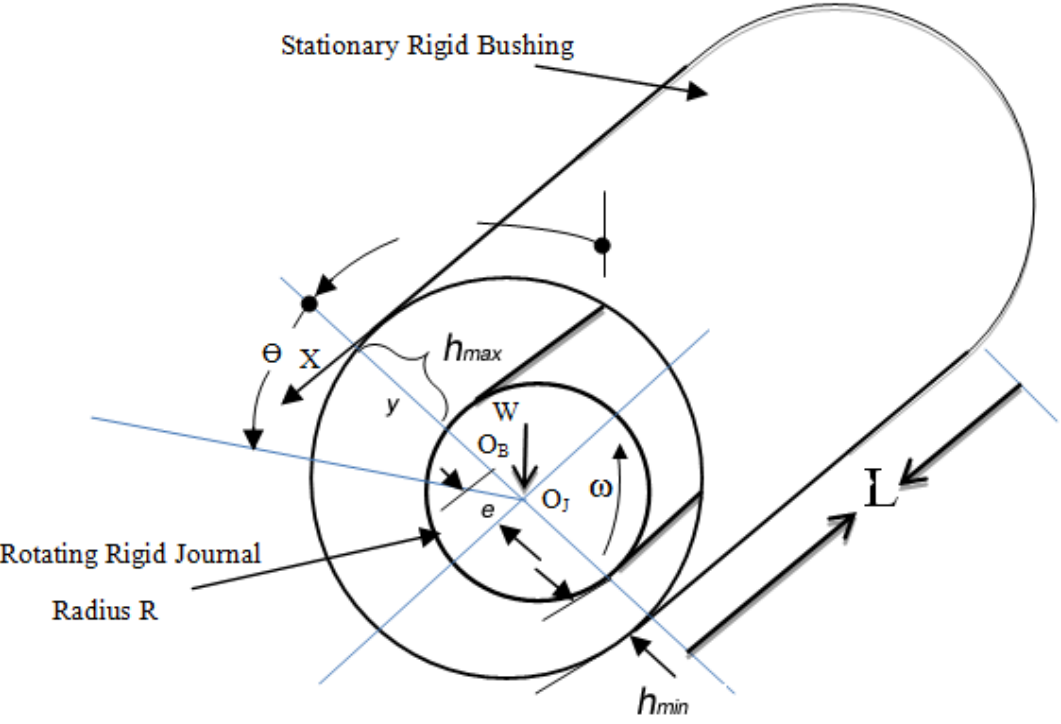
Figure 1.3: Scheme of the examined bearing

1.1 Literature Review

Wear is the major cause of material wastage and loss of mechanical performance of machine elements. Reduction in wear can result in considerable savings which can be made by improved friction control. Lubrication is an effective means of controlling wear and reducing friction, and it has wide applications in the operation of machine elements such as bearings. The principles of hydrodynamic lubrication were first established by a well-known scientist Osborne Reynolds in 1886 and he explained the mechanism of hydrodynamic lubrication through the generation of a viscous liquid film between the moving surfaces.

The journal bearing design parameter such as load capacity can be determined from Reynolds equation both analytically and numerically (Hamrock, 1994). Saynatjoki and Holmberg (1982) described a magnetic fluid as not a simple fluid; it is a stable suspension of small particles of ferromagnetic materials in a base fluid. For the purpose of ensuring the colloid stability, a surfactant of polymers (such as oleic acid) is usually introduced into the suspension. This will create around each single particle a coating layer to prevent the agglomeration of the particles by the magnetic field effect or by the molecular attraction. When a magnetic field is applied to the magnetic fluid, each particle experiences a force that depends on the magnetization of the magnetic material of the particles and on the strength of the applied field.

The effects of variable density and variable specific heat on maximum pressure, maximum temperature, bearing load, frictional loss and side leakage in high-speed journal bearing operation were examined by Chum, (2004). Regarding the preparations of Ferro fluids and the properties of these magnetic fluids, a lot of literature is available according to Rosensweig *et al* (1969), Rosensweing (1982) and Raj *et al* (1987).

8

Presently, lubricating oils often contain some additives of high-molecular-weight polymers to modify some physical (pour point, foaming, or viscosity temperature behavior) and chemical properties (oxidation, detergency, or corrosion). These additives are long-chain organic compounds; e.g., the length of the polymer chain may be a million times the diameter of a water molecule. Due to this special structure of the magnetic-lubricant fluid and also due to the other additives, the Newtonian fluid approximation (which neglects the size of fluid particles) is not a satisfactory engineering approach.

A number of micro-continuum theories have been developed according to Ariman *et al* (1973) and Ariman *et al* (1974) for describing the peculiar behavior of fluids containing substructures, which can translate, rotate, or even deform independently. Among them, the Stokes micro-continuum theory (Stokes, 1966) is the simplest theory that allows for polar effects such as the presence of couple stresses and body couples. These couple stresses may be significant particularly under lubrication conditions where thin films usually exist.

A number of studies have applied the Stokes micro continuum theory to investigate the effect of couple stresses on the performance of different types of fluid-film bearings. Based on the stokes micro continuum theory, the problem of lubrication of finite hydrodynamic journal bearing lubricated by magnetic fluids with couple stresses was investigated (Arima and Sylvester, 1973) and by including these couple stresses due to micro structure additives and the magnetic effects due the magnetization of the magnetic fluid, the modified Reynolds equation was obtained to study bearing characteristics. The studies cited above consider the magnetic fluid to behave as a Newtonian fluid but other researches treated the magnetic fluid as non- Newtonian fluid using the power-law model according to Osman (1999), Osman *et al* (2002) and Osman *et al* (2003).

Investigation on the lubrication of lightly loaded cylinders in combined rolling, sliding, and normal motion with a couple stress fluids as lubricant under cavitation boundary conditions was

done by Bujurke and Naduvinamani (1990). They noted that the load capacity and the frictional drag increased as the squeeze velocity increased. Increasing the couple stress parameter enhanced this increase. Presentation on the study of performance of finite journal bearings lubricated with a fluid with couple stresses taking into account the elastic deformation of the liner have been done by Mokhiamer *et al* (1999). They concluded that the influence of couple stresses on the bearing characteristics was significantly apparent.

Study on the static characteristics of rotor bearing systems lubricated with couple stress fluids with the effect of surface roughness considerations have been done clearly by Naduvinamani *et al* (2002). They formulated and solved for transverse and longitudinal roughness for these problem. Nada and Osman (2007) investigated the static performance of finite hydrodynamic journal bearings lubricated by magnetic fluids with couple stresses and among their conclusion was that the magnetic lubricant gives higher load carrying capacity, higher attitude angle, lower friction coefficient, and higher side leakage. These effects are more significant where the hydrodynamic effects are low, at the lower values of couple stress parameter and eccentricity ratios.

Fundamentals of fluid film Journal bearing operation and modeling were reviewed in a turbo machinery symposium by Minhui *et al,* (2005). Their work provided practical knowledge on the basic operation and what physical effects should be included in modeling a bearing so as to help ensure reliable operation in the field. They reviewed all the important theoretical aspects of journal bearing modeling, such as film pressure, film and pad temperatures, thermal and mechanical deformations, and turbulent flow.

Thermal effects on hydrodynamic journal bearings lubricated by magnetic fluids and with couple stresses were studied by Abdo *et al* (2009). They concluded that the magnetic lubrication gives higher pressure distribution, with small insignificant fluid temperature rise. The load carrying

capacity increases without increase of the friction force. They also found that the magnetic lubrication has decreased the effect of the side leakage such that the bearing may operate without any side leakage. Taking into account of the couple force their results shown that lubricants with couple stresses compared with Newtonian lubricants increase the pressure and temperature especially at high eccentricity ratios. The couple stresses give increase in both load carrying capacity and friction force and decrease in friction coefficient. Thus it can be concluded that fluids with couple stresses are better than Newtonian fluids.

Numerical analysis has allowed models of hydrodynamic lubrication to include closer approximations to the characteristics of real bearings. Numerical solutions to hydrodynamic lubrication problems can now satisfy most engineering requirements for prediction of bearing characteristics. To analyze the bearing design parameters, several approximate numerical methods have evolved over the years such as the finite difference method and the finite element method. Finite element method has been used for the solution of the hydrodynamic lubrication problem to obtain bearing traits by Booker and Huebner (1972).

Nessil *et al,* (2012) did an analysis of journal bearings lubrication using non-Newtonian fluids which they described by a power-law model. They determined the performance characteristics of the journal bearings for various values of the non-Newtonian power-law index "n". The numerical results they obtained showed that for the dilatant fluids ($n > 1$), the load-carrying capacity, the pressure, the temperature, and the frictional force increased while for the pseudo-plastic fluids ($n < 1$) they decreased. Thermo-hydrodynamic analysis of a Journal bearing using CFD as a tool was done by Mukesh *et al,* (2012). From the results they obtained, it was clear that temperature created from the frictional force increase as the viscosity of the lubricant decrease and lesser viscosity decreases the maximum pressure of the lubricant inside the bearing.

Priyanka and Veerendra, (2012) reviewed the analysis of hydrodynamic journal bearing and in their work they presented a survey of important papers pertaining to analysis of various types of methods, equations and theories used for the determination of load carrying capacity, minimum oil film thickness, friction loss, and temperature distribution of hydrodynamic journal bearing. Predictions of these parameters are the very important aspects in the design of hydrodynamic journal bearings. They focused on various types of factors which tremendously affect the performance of hydrodynamic journal bearing. They found that friction coefficient is increased, with increasing wear depth as well as misalignment and Sommerfeld number. The friction coefficient and consequently the power loss are strongly dependent upon the misalignment angle and wear depth. The noise of the bearing decreases as the mass eccentricity of the rotor decreases, the lubricant viscosity increases, the width of the bearing increases, and the radial clearance of the bearing decreases.

Calvalca and, Daniel (2013) evaluated the thermal effects in tilting pad bearing where their results showed that the temperature increases as the rotational speed increases due to the shear rate of the oil film. The maximum temperature in the bearing occurred in the overloaded pad, near the outlet boundary. They performed experimental tests in a tilting pad journal bearing operating in a steam turbine to validate the model. Comparing the experimental and numerical results they provided a good correlation. They finally concluded that the thermo-hydrodynamic lubrication as developed in their work is promising to consistently evaluate the behavior of the tilting pad journal bearing operating in relatively high rotational speeds.

In our departure, we therefore seek to investigate the effect of the parameters such as the eccentricity ratio, magnetic coefficient and couple forces parameter that affect the characteristics of journal bearing and discuss the velocity and temperature distributions in relation to the referred parameters.

12

1.2 Problem statement

Journal bearing operates effectively and more efficiently when it is in hydrodynamic case where there is no contact between the parts of the journal bearing surfaces. Oil have been used mostly as the lubricant in the past but with more research it was discovered that magnetic lubricant gives higher load carrying capacity, higher attitude angle and lower friction coefficient. These effects are more significant where the hydrodynamic effects are low, at the lower values of couple stress parameter and eccentricity ratios. It has been concluded that fluids with microstructures are better lubricant than Newtonian fluids especially if they were prepared to become magnetic fluids (Nada and Osman, 2007). We therefore seek to investigate the effect of the parameters such as the eccentricity ratio, magnetic coefficient and couple forces parameter that affect the characteristics of an elasto-hydrodynamic journal bearing and discuss the velocity and temperature distributions in relation to the referred parameters. We also determine the effect of Joules heating to the Journal bearing.

1.3 Justification

Equipment's and machines with rotating parts are commonly used in our society for a wide range of energy conservation applications such as automobiles, electric power generation, cooling and ventilation systems. Therefore there is need to design a long lasting and efficient bearing and be in a position to control different parameter effects that would affect the bearing characteristics. Journal bearing operates effectively and more efficiently when it is a full fluid film where there is no contact between the parts of the journal bearing surfaces. In real life we have no such a case where there is absolutely no contact and therefore we investigate the effects of such parameters that would affect an Elasto-hydrodynamic journal bearing performance.

1.4 Hypothesis

The load carrying capacity of the bearing will not decrease due to the use of a non-conductive magnetic fluid. The hypothesis null is since in this study since the results obtained gives a different conclusion that the pressure increases for a magnetic fluid thus the load carrying capacity increases contradicting the hypothesis.

1.5 Objectives

1.5.1 General Objective

Determination of the static performance of finite elasto-hydrodynamic journal bearings lubricated by magnetic fluids with couple stresses

1.5.2 Specific Objectives

a. To determine the velocity profiles, skin frictions and the rate of mass transfer in a hydro magnetic journal bearing.

b. To determine the pressure and temperature profiles.

c. To determine the effect of eccentricity ratio, magnetic parameter and the couple force parameter on an elasto-hydrodynamic journal bearing performance.

CHAPTER TWO

2.0 INTRODUCTION

This chapter is concerned with the equations that govern the study of Magneto Hydrodynamic flows. The continuity, momentum, induction and the energy equations are discussed. Towards the end of the chapter, the method of solution is introduced.

2.1 THE GOVERNING EQUATIONS

The governing equations are those that assist us in the analysis of the journal bearing which forms the basis of our interest. We therefore look at a number of these equations;

2.1.1 Equation of Conservation of Mass

The equation of conservation of mass is also called the equation of continuity. It is derived from the law of conservation of mass. The law of conservation of mass states that mass can neither be created nor destroyed, i.e. given a steady flow process, the stored mass in a control volume does not change. Steady flow process is a process where the flow rate does not change with time. This means that inflow into a control volume equals to the outflow. The general equation of continuity is expressed as;

$$\frac{\partial \rho}{\partial t} + \frac{\partial (\rho u_i)}{\partial x_i} = 0 \qquad (2.1)$$

For a steady and incompressible fluid flow, the tensor form of the equation of continuity is given as;

$$\frac{\partial u_i}{\partial x_i} = 0 \qquad (2.2)$$

2.1.2 Equation of Conservation of Momentum

The law of conservation of momentum states that the rate of change of momentum in the control volume is equal to the sum of the net momentum flux into the control volume and any external forces acting on the control volume this is as a result of Newton second law of motion. This means that the total momentum of a closed system is constant. The general momentum equation in tensor form is expressed as;

$$\rho\left(\frac{\partial u_i}{\partial t}+u_j\frac{\partial u_i}{\partial x_j}\right)=\vec{\nabla}P+\upsilon\nabla^2 u_i+\rho F_i \tag{2.3}$$

2.1.3 Equation of Induced Magnetic Force

The induced magnetic force for the magnetic fluid under the effect of magnetic field is given by (Cowley and Rosensweig 1967, Zelazo and Melcher 1969)

$$\vec{F}_m=\left(\vec{\nabla}\times h_m\right)\times\vec{B}+\mu M_g\left(\vec{\nabla}h_m\right) \tag{2.4}$$

Where $\vec{B}$ is the magnetic field density vector and $\left(\vec{\nabla}\times h_m\right)$ represents the induced free current and M_g is magnetization of the magnetic material. This force will be used in the equation of motion as an external body force.

2.1.4 Reynolds Equation

The Reynolds equation is derived from the Navier Stokes equation where the velocities obtained are substituted into the continuity equation and then integrated across the fluid film thickness $\left(0\le y\le h(x,z)\right)$. According to (Hamrock, 1994) the Reynolds equation derived is applicable for Elasto-hydrodynamic lubrication. The general Reynolds equation in standard form as was derived by (Hamrock, 1994) is as given in equation 2.5;

16

$$\frac{\partial}{\partial x}\left(\frac{\rho h^3}{\mu}\frac{\partial P}{\partial x}\right) + \frac{\partial}{\partial y}\left(\frac{\rho h^3}{\mu}\frac{\partial P}{\partial y}\right) = 12\left(\frac{u_a + u_b}{2}\right)\frac{\partial(\rho h)}{\partial x} + 12\left(\frac{v_a + v_b}{2}\right)\frac{\partial(\rho h)}{\partial y} \qquad (2.5)$$

2.2 PROBLEM MODELING

2.2.1 Magnetic Force Calculations

For a Ferro-fluid under a magnetic field, from equation (2.4) the induced magnetic force is reduced to our specific case as Illustrated;

$$\vec{F}_m = \left(\vec{\nabla} \times h_m\right) \times B + \mu_0 M_g\left(\vec{\nabla} h_m\right) \qquad (2.6)$$

Where $\vec{B}$ is the magnetic field density vector and $(\vec{\nabla} \times h_m)$ represents the induced free current. Since the electrical properties of the Ferro-fluid are similar to that of the base fluid, they are non-conductive (except where there is a metallic base fluid) and no free currents are induced. The first term therefore, can be cancelled and the equation is rewritten as

$$F_m = \mu_0 M_g\left(\vec{\nabla} h_m\right) \qquad (2.7)$$

The magnetization can be regarded only dependent on the applied field. The magnetization under this condition can be roughly divided into two parts as used by Abdo *et al*, 2009.

1. If an applied magnetic field is strong enough; the magnetization of the fluid reaches a saturation state and is almost constant, *Mg=Mgs*, and the induced magnetic force is given by:

$$F_m = \mu_0 M_{gs}\left(\vec{\nabla} h_m\right) \qquad (2.8)$$

2. If a small or moderate applied field is applied; the magnetization of the fluid is approximately proportional to the applied field. $M_g = X_m\, h_m$, and the induced magnetic force is given by:

$$F_m = \mu_0 X_m h_m\left(\vec{\nabla} h_m\right) \qquad (2.9)$$

17

In this study, the second case is assumed and is used as a body external force in the flow field.

2.2.2   Modified Reynolds Equation

From stokes micro-continuum theory, the field equations of an incompressible fluid with couple stress gives that the general equation of momentum becomes equation 2.10. Thus the equation is broken down in the respective directions.

$$\rho \frac{D\vec{q}}{Dt} = -\nabla P + F_m + \frac{1}{2} \nabla \times B + \left(\mu - \eta \nabla^2 \right) \nabla^2 \vec{q} \tag{2.10}$$

In x direction

$$\rho \left(\frac{\partial u}{\partial t} + u \frac{\partial u}{\partial x} \right) = -\frac{\partial P}{\partial x} + F_{mx} + \mu \frac{\partial^2 u}{\partial x^2} - \eta \frac{\partial^4 u}{\partial x^4} \tag{2.11}$$

In y direction

$$\rho \left(\frac{\partial v}{\partial t} + v \frac{\partial v}{\partial y} \right) = -\frac{\partial P}{\partial y} + F_{my} + \mu \frac{\partial^2 v}{\partial y^2} - \eta \frac{\partial^4 v}{\partial y^4} \tag{2.12}$$

In z direction

$$\rho \left(\frac{\partial w}{\partial t} + w \frac{\partial w}{\partial z} \right) = -\frac{\partial P}{\partial z} + F_{mz} + \mu \frac{\partial^2 w}{\partial z^2} - \eta \frac{\partial^4 w}{\partial z^4} \tag{2.13}$$

Where:

F_{mx}, F_{my} and F_{mz} are the components of external forces per unit volume. $\rho \left(\frac{\partial u}{\partial t} + u \frac{\partial u}{\partial x} \right)$,

$\rho \left(\frac{\partial v}{\partial t} + v \frac{\partial v}{\partial y} \right)$ and $\rho \left(\frac{\partial w}{\partial t} + w \frac{\partial w}{\partial z} \right)$ are the three components of acceleration of the fluid.

Equations (2.11) to (2.13) contain the four unknowns' *u, v, w* and *p*. The fourth equation is given by the continuity equation to be able to solve for the unknowns:

$$\frac{\partial u}{\partial x} + \frac{\partial v}{\partial y} + \frac{\partial w}{\partial z} = 0 \qquad (2.14)$$

Using the assumptions below;

1. The lubricant is assumed to be a Newtonian fluid.

2. The flow is laminar; consequently, neither vortex flow nor turbulence is occurring anywhere in the flow.

3. The lubricant is assumed incompressible; i.e. its density is constant.

4. The curvature of the fluid film is neglected since the film thickness in y-direction is very thin compared with the span in x and z-directions. Thus, no gradient of the applied magnetic field across the fluid film, no magnetic force in y-direction and thus no pressure gradient in this direction $\frac{\partial P}{\partial y} = 0$

5. The fluid flow is steady, implying that $\frac{\partial u}{\partial t} = \frac{\partial y}{\partial t} = \frac{\partial w}{\partial t} = 0$

6. The fluid inertia force is neglected compared to the viscous force and the induced magnetic force

7. No-slip condition exists at the bearing surface.

8. Except $\frac{\partial u}{\partial y}$ and $\frac{\partial w}{\partial y}$, all other velocity gradients are considered negligible.

9. No heat conducted to or from the fluid film to surfaces (adiabatic case).

The assumptions and approximations are necessary so as to reduce the equations in a way they could suit a natural phenomenon. Therefore the momentum equations can be written as;

$$\frac{\partial P}{\partial x} = F_{mx} + \mu \frac{\partial^2 u}{\partial y^2} - \eta \frac{\partial^4 u}{\partial y^4} \tag{2.15}$$

$$\frac{\partial P}{\partial y} = 0 \tag{2.16}$$

$$\frac{\partial P}{\partial z} = F_{mz} + \mu \frac{\partial^2 w}{\partial y^2} - \eta \frac{\partial^4 w}{\partial y^4} \tag{2.17}$$

Where F_{mx} and F_{mz} are the magnetic force components in circumferential and axial directions respectively.

The boundary conditions can be stated as below;

At $y = 0$ $\qquad\qquad\qquad u = 0 \;\; v = 0 \;\; w = 0$ $\qquad\qquad$ (2.18)

$$\frac{\partial^2 u}{\partial y^2} = 0 \;\;,\;\; \frac{\partial^2 w}{\partial y^2} = 0 \tag{2.19}$$

At $y = \dfrac{h}{2}$ $\qquad\qquad u = \dfrac{\omega \Re}{h}, \;\; v = 0 \;\; w = 0$ $\qquad\qquad$ (2.20)

$$\frac{\partial u}{\partial y} = 0 \;\;,\;\; \frac{\partial w}{\partial y} = 0 \tag{2.21}$$

At $y = h$ $\qquad\qquad\qquad u = \omega \Re, \;\; v = 0 \;\; w = 0$ $\qquad\qquad$ (2.22)

$$\frac{\partial^2 u}{\partial y^2} = 0 \;\;,\;\; \frac{\partial^2 w}{\partial y^2} = 0 \tag{2.23}$$

Equations (2.18), (2.20) and (2.22) are the no slip boundary conditions. Equations (2.19), (2.21) and (2.23) result from the couple stress and vanish at the solid surfaces (Nada and Osman, 2007). This is due to the resistance of the solid surfaces for the rotation motion of the additive particles

By solving equations (2.15) and (2.17) analytically and using the above boundary conditions, the velocity profiles in circumferential and axial directions are obtained as below (Nada and Osman, 2007).

$$u = \omega \Re \frac{y}{h} + \frac{1}{2\mu}\left(\frac{\partial P}{\partial x} - F_{mx}\right) \times \left[\left(y^2 - yh\right) + 2l^2\left\{1 - \frac{\cosh\left(\frac{2y-h}{2l}\right)}{\cosh\left(\frac{h}{2l}\right)}\right\}\right] \tag{2.24}$$

$$w = \frac{1}{2\mu}\left(\frac{\partial P}{\partial z} - F_{mz}\right) \times \left[\left(y^2 - yh\right) + 2l^2\left\{1 - \frac{\cosh\left(\frac{2y-h}{2l}\right)}{\cosh\left(\frac{h}{2l}\right)}\right\}\right] \tag{2.25}$$

Where $l = \left(\frac{\eta}{\mu}\right)^{\frac{1}{2}}$ \hfill (2.26)

These velocities are substituted in the following integrated continuity equation across the fluid film thickness for an incompressible fluid flow and then solved to give the specific Reynolds equation.

$$\int_0^h \left(\frac{\partial u}{\partial x} + \frac{\partial v}{\partial y} + \frac{\partial w}{\partial z}\right) dy = 0 \tag{2.27}$$

Solving this integral equation 2.28 is obtained;

$$\frac{\omega \Re}{2}\frac{\partial h}{\partial x} - \frac{1}{12\mu}\frac{\partial}{\partial x}\left[\left(h^3 - 12l^2 h + 24l^3 \tanh\left(\frac{h}{2l}\right)\right)\frac{\partial P}{\partial x}\right] + \frac{1}{12\mu}\frac{\partial}{\partial x}\left[\left(h^3 - 12l^2 h + 24l^3 \tanh\left(\frac{h}{2l}\right)\right)F_{mx}\right]$$

$$- \frac{1}{12\mu}\frac{\partial}{\partial z}\left[\left(h^3 - 12l^2 h + 24l^3 \tanh\left(\frac{h}{2l}\right)\right)\frac{\partial P}{\partial z}\right] + \frac{1}{12\mu}\frac{\partial}{\partial z}\left[\left(h^3 - 12l^2 h + 24l^3 \tanh\left(\frac{h}{2l}\right)\right)F_{mz}\right] = 0 \tag{2.28}$$

Rearranging this equation we have;

$$\frac{1}{12\mu}\frac{\partial}{\partial x}\left[\left(h^3 - 12l^2 h + 24l^3 \tanh\left(\frac{h}{2l}\right)\right)\frac{\partial P}{\partial x}\right] + \frac{1}{12\mu}\frac{\partial}{\partial x}\left[\left(h^3 - 12l^2 h + 24l^3 \tanh\left(\frac{h}{2l}\right)\right)F_{mx}\right] = \frac{\omega\Re}{2}\frac{\partial h}{\partial x}$$

$$+\frac{1}{12\mu}\frac{\partial}{\partial z}\left[\left(h^3 - 12l^2 h + 24l^3 \tanh\left(\frac{h}{2l}\right)\right)\frac{\partial P}{\partial z}\right] + \frac{1}{12\mu}\frac{\partial}{\partial z}\left[\left(h^3 - 12l^2 h + 24l^3 \tanh\left(\frac{h}{2l}\right)\right)F_{mz}\right] \quad (2.29)$$

This equation can be re-written as;

$$\frac{\partial}{\partial x}\left(\frac{g(h,l)}{\mu}\frac{\partial P}{\partial x}\right) + \frac{\partial}{\partial z}\left(\frac{g(h,l)}{\mu}\frac{\partial P}{\partial z}\right) = 6\omega\Re\frac{\partial h}{\partial x} + \frac{\partial}{\partial x}\left(\frac{g(h,l)}{\mu}F_{mx}\right) + \frac{\partial}{\partial z}\left(\frac{g(h,l)}{\mu}F_{mz}\right) \quad (2.30)$$

Where;

$$g(h,l) = h^3 - 12l^2 h + 24l^3 \tanh\left(\frac{h}{2l}\right) \quad (2.31)$$

Substituting equation (2.9), the components of magnetic force (F_{mx} and F_{mz}) can be obtained in the x and z directions respectively as below;

$$F_{mx} = \mu_0 X_m h_m \frac{\partial h_m}{\partial x} \quad (2.32)$$

$$F_{mz} = \mu_0 X_m h_m \frac{\partial h_m}{\partial z} \quad (2.33)$$

Substituting equations (2.32) and (2.33) in the Reynolds equation (2.30) above we obtain;

$$\frac{\partial}{\partial x}\left(\frac{g(h,l)}{\mu}\frac{\partial P}{\partial x}\right) + \frac{\partial}{\partial z}\left(\frac{g(h,l)}{\mu}\frac{\partial P}{\partial z}\right) = 6\omega\Re\frac{\partial h}{\partial x} + \frac{\partial}{\partial x}\left(\frac{g(h,l)}{\mu}\mu_0 X_m h_m \frac{\partial h_m}{\partial x}\right) + \frac{\partial}{\partial z}\left(\frac{g(h,l)}{\mu}\mu_0 X_m h_m \frac{\partial h_m}{\partial z}\right)$$

$$(2.34)$$

Considering the general equation of energy and taking in to account the magneto elasto-hydrodynamics, the specific energy equation is obtained,

$$\rho C_v \frac{DT}{Dt} = k\nabla^2 T + \mu\phi + \frac{1}{\sigma}J^2 \quad (2.35)$$

The energy equation is changed due to electric dissipation which is the heat energy produced by the work done by electric current. The electric dissipation is referred to as the joule's heating and is given as $\frac{1}{\sigma}J^2$. The term $\mu\phi$ is the internal heating due to viscous dissipation. For an incompressible fluid flow, viscous dissipation function ϕ in three dimensions is expressed as;

$$\phi = 2\left[\left(\frac{\partial u}{\partial x}\right)^2 + \left(\frac{\partial v}{\partial y}\right)^2 + \left(\frac{\partial w}{\partial z}\right)^2\right] + \left[\left(\frac{\partial u}{\partial y} + \frac{\partial v}{\partial x}\right)^2 + \left(\frac{\partial v}{\partial z} + \frac{\partial w}{\partial y}\right)^2 + \left(\frac{\partial w}{\partial x} + \frac{\partial u}{\partial z}\right)^2\right] - \frac{2}{3}\left(\frac{\partial u}{\partial x} + \frac{\partial v}{\partial y} + \frac{\partial w}{\partial z}\right)^2 \qquad (2.36)$$

The term $\left(\frac{\partial u}{\partial x} + \frac{\partial v}{\partial y} + \frac{\partial w}{\partial z}\right)$ reduces to zero since it represents the equation of continuity. The partial derivatives of v; such as $\frac{\partial v}{\partial x}, \frac{\partial v}{\partial y}$ and $\frac{\partial v}{\partial z}$ vanishes since all are equal to zero. The bearing is parallel to the x-axis, and therefore the contribution of the terms $\frac{\partial u}{\partial x}$ and $\frac{\partial w}{\partial x}$ to viscous dissipation is assumed to be negligible and the terms are therefore dropped from the equation. Also, the z-axis is infinite and thus the partial derivatives with respect to z are dropped from the equation. Therefore, the viscous dissipation equation reduces to;

$$\phi = 2\left[\left(\frac{\partial u}{\partial y}\right)^2 + \left(\frac{\partial w}{\partial y}\right)^2\right] \qquad (2.37)$$

2.2.3   Using the Electromagnetic equations

Maxwell's equations

The Maxwell's equations give the relation between the interacting electric and magnetic fields. Maxwell's equations consist of fundamental electromagnetic equations for time varying magnetic field and these equations are listed as equation 2.38 to equation 2.41.

$$\nabla \times E = -\frac{\partial B}{\partial t} \qquad \text{Or} \qquad \nabla \times E = \mu \frac{\partial H}{\partial t} \tag{2.38}$$

$$\nabla \times H = J + \frac{\partial D}{\partial t} \tag{2.39}$$

$$\nabla \cdot D = \rho_e \tag{2.40}$$

$$\nabla \cdot B = 0 \tag{2.41}$$

Equation (2.38) is the Faraday's law that was named after Michael Faraday, who in 1831, experimentally discovered that a current is induced in a conducting loop when magnetic flux linking the loop changes. It is an experimental law and can be considered as an axiom (truth without proof). This equation expresses an axiom for electromagnetic induction which means that the electric field intensity in a region of time varying magnetic flux density is non-conservative and cannot be expressed as a gradient or scalar potential.

Equation (2.39) is the Ampere's law that was named after Ampere Andre-Marie, and which states that wires carrying electric currents attract and repel each other magnetically.

Form Maxwell's electromagnetic equations, the relation $\nabla \cdot B = 0$ yields $\frac{\partial B}{\partial y} = 0$. When the magnetic Reynolds number is small, induced magnetic field is negligible in comparison with the applied magnetic field. This therefore leads to;

$B_x = B_z = 0$ and that $B_y = B_0$ (a constant)

The current density **J** has the components $\left(J_x, J_y, J_z\right)$. Therefore, the equation of conservation of electric charge $\nabla \cdot J = 0$ where it gives that;

24

J_y = a constant

Since the bearing wall is non-conducting, $J_y = 0$ at the bearing wall and hence it becomes zero everywhere in the flow. Neglecting the polarization effect, the electric field $\mathbf{E} = 0$. Therefore giving

$$J = (J_x, 0, J_z), \ B = (0, B_0, 0) \text{ and } q = (u, v, w) \tag{2.42}$$

The general Ohms law is expressed as;

$$J = \sigma(E + q \times B) \tag{2.43}$$

The magnetic field is considered to act only from one direction (divergence less). This means that there are no magnetic flux sources and sinks within the field, and therefore $\nabla \cdot B = 0$. The mathematical expression of the continuity equation in the case of conservation of electric charge becomes;

$$\nabla \cdot J = -\frac{\partial \rho_e}{\partial t} \tag{2.44}$$

The term $q \times B$ in equation (2.43) thus yields equation 2.45

$$q \times B = \begin{vmatrix} i & j & k \\ u & v & w \\ 0 & B_0 & 0 \end{vmatrix} = -wB_0 i + uB_0 k \tag{2.45}$$

Therefore, from equations (2.43) and (2.45) gives the x-axis and z-axis components of the current density which reduces to equation 2.46.

$$J_x = -\sigma w B_0 \text{ and } J_z = \sigma u B_0 \tag{2.46}$$

Now, the Lorentz force $J \times B$ is expressed as equation 2.47.

$$J \times B = \begin{vmatrix} i & j & k \\ -\sigma w B_0 & 0 & \sigma u B_0 \\ 0 & B_0 & 0 \end{vmatrix} = -\sigma u B_0^2 i - \sigma w B_0^2 k \tag{2.47}$$

Heat generated due to electrical resistance of the fluid to the flow of the induced electric current is given as the joule heating which yields equation 2.48;

$$\frac{J^2}{\sigma} = \sigma w^2 B_0^2 + \sigma u^2 B_0^2 = \sigma B_0^2 \left(u^2 + w^2 \right) \tag{2.48}$$

Taking viscous dissipation (2.37) and the joules heating (2.48) into considerations the equation of energy is as in equation 2.49.

$$\rho C_p \left(\frac{\partial T}{\partial t} + u \frac{\partial T}{\partial x} + w \frac{\partial T}{\partial z} \right) = k \left(\frac{\partial^2 T}{\partial x^2} + \frac{\partial^2 T}{\partial z^2} \right) + 2\mu \left[\left(\frac{\partial u}{\partial y} \right)^2 + \left(\frac{\partial w}{\partial y} \right)^2 \right] + \sigma B_0^2 \left(u^2 + w^2 \right) \tag{2.49}$$

2.2.4   Magnetic field model

The magnetic model used is according to Abdo *et al*, (2009) where a concentric finite wire was placed at the center of the shaft and some current passed through. Therefore, induced magnetic field is produce by the effect of the current passing through the wire according to Maxwell's equations. The produced magnetic field is represented by equation (2.50);

$$h_m(z) = \frac{I}{4\pi R} \left(\sin\left(\tan^{-1}\left\{ \frac{L/2 + z}{R} \right\} \right) + \sin\left(\tan^{-1}\left\{ \frac{L/2 - z}{R} \right\} \right) \right) \tag{2.50}$$

This equation in non-dimensionalzed form is expressed as equation (2.51);

$$H_m(Z) = \sin\left\{\tan^{-1}(\beta + 2\beta Z)\right\} + \sin\left\{\tan^{-1}(\beta - 2\beta Z)\right\} \tag{2.51}$$

Where, $h_{mo} = \dfrac{I}{4\pi R}$, and is the characteristic value of magnetic field intensity

Thus, substituting equation (2.51) in the modified Reynolds and the specific Energy equations, our model is now ready to be solved numerically simultaneously and the effect of this model on the overall bearing characteristics can be achieved.

2.2.5 Bearing Geometry and Boundary Conditions

The considered bearing is an axial feeding cylindrical finite journal bearing. It is schemed as in Figure 1.3. The geometric axes of the journal and bearing are assumed parallel. The arc length (θ) from the oil admission line and considering maximum clearance median section, the film thickness is given as equation (2.52),

$$h = C + eCos\theta \tag{2.52}$$

Where, e is the eccentricity ratio

Equation (2.52) in non-dimensional form it is expressed as equation (2.53)

$$H = 1 + \varepsilon Cos\theta \tag{2.53}$$

Where, ε is the non-dimensionalzed eccentricity ratio.

The film thickness H depends totally on the change of the angle θ and hence the derivatives of H with respect to θ remains while those of Hm with respect to θ vanishes. Considering the boundary conditions, it is clear that the pressure and the temperature are symmetrical about the middle plane of the bearing $(Z = 0)$. Thus one half of the bearing would reflect the other.

The boundary conditions used are;

$P(0, Z) = P(2\pi, Z) = 0$ At the line of lubricant admission

$P(\theta, -0.5) = P(\theta, 0.5) = 0$ At the bearing ends

$$\frac{\partial P}{\partial Z}(\theta,0,0)=0 \qquad \text{This due to the bearing symmetry}$$

For the temperature;

$$T(0,0,Z)=0 \qquad \text{At the lone of lubricant admission}$$

$$T(\theta,-0.5)=T(\theta,0.5)=0 \qquad \text{At the bearing ends}$$

2.3 NON-DIMENSIONALIZATION

The principal use of dimensional analysis is to deduce from a study of the dimensions of the variables in any physical system certain limitations on the form of any possible relationship between those variables. The method is of great generality and mathematical simplicity. This is a process that starts with selecting a suitable scale against which all dimensions in a given physical model are scaled. This process aims at ensuring that the results obtained are applicable to other geometrically similar configurations under similar set of flow conditions. The dimensionless quantities are introduced as below;

$$x=R\theta \,, z=L_b Z \,,\quad e=C\varepsilon \,, h=CH \,, l=CL \,,\quad L_b=2R\beta \,,\quad h_m=h_{mo}H \text{ and } P=\frac{\lambda_0 \omega P^*}{(C/R)^2}$$

Introducing these non-dimensional quantities to equation (2.34) the modified Reynolds equation 2.54 is achieved;

$$\frac{\partial}{\partial\theta}\left(G(H,L)\frac{\partial P^*}{\partial\theta}\right)+\frac{1}{4\beta^2}\frac{\partial}{\partial z}\left(G(H,L)\frac{\partial P^*}{\partial z}\right)=6\frac{\partial H}{\partial\theta}+4\beta^2\alpha\frac{\partial}{\partial\theta}\left(G(H,L)H_m\frac{\partial H_m}{\partial\theta}\right)+\alpha\frac{\partial}{\partial z}\left(G(H,L)H_m\frac{\partial H_m}{\partial z}\right) \qquad (2.54)$$

Where $G(H,L)=H^3-12L^2H+24L^3\tanh\left(\frac{H}{2L}\right)$ and $\alpha=\frac{(h_{mo})^2\lambda_0 X_m C^2}{\mu_0\omega(L_b)^2}$

It is noted that, as the value of (L) tend to zero, equation (2.54) is reduced to the Newtonian magnetic lubricant case and the effect of couple stresses vanishes as shown in equation (2.55).

$$\frac{\partial}{\partial\theta}\left(H^3\frac{\partial P^*}{\partial\theta}\right)+\frac{1}{4\beta^2}\frac{\partial}{\partial z}\left(H^3\frac{\partial P^*}{\partial z}\right)=6\frac{\partial H}{\partial\theta}+4\beta^2\alpha\frac{\partial}{\partial\theta}\left(H^3H_m\frac{\partial H_m}{\partial\theta}\right)+\alpha\frac{\partial}{\partial z}\left(H^3H_m\frac{\partial H_m}{\partial z}\right) \qquad (2.55)$$

To non-dimensionalize the specific energy equation (2.49), the non-dimensional quantities used were,

$$x=R\theta, \quad y=Cy^*, \quad z=L_bZ, \quad t=\frac{Ht^*}{U_\infty}, \quad T=T^*(T_w-T_\infty)+T_\infty, \quad u=u^*U_\infty, \text{ and } w=w^*U_\infty$$

To non-dimensionalize this equation the following operations were first carried out to the non-dimensional parameters labeled as equations 2.56(a), (b), (c), (d), (e), (f) and (g).

$$\frac{\partial T}{\partial t}=\frac{\partial T}{\partial T^*}\cdot\frac{\partial T^*}{\partial t^*}\cdot\frac{\partial t^*}{\partial t}=\frac{U_\infty(T_w-T_\infty)}{C}\frac{\partial T^*}{\partial t^*} \qquad 2.56(a)$$

$$u\frac{\partial T}{\partial x}=u^*U_\infty\frac{\partial T}{\partial T^*}\cdot\frac{\partial T^*}{\partial\theta}\cdot\frac{\partial\theta}{\partial x}=\frac{U_\infty(T_w-T_\infty)}{R}u^*\frac{\partial T^*}{\partial\theta} \qquad 2.56(b)$$

$$w\frac{\partial T}{\partial z}=w^*U_\infty\frac{\partial T}{\partial T^*}\cdot\frac{\partial T^*}{\partial Z}\cdot\frac{\partial Z}{\partial z}=\frac{U_\infty(T_w-T_\infty)}{L_b}w^*\frac{\partial T^*}{\partial Z} \qquad 2.56(c)$$

$$\frac{\partial^2 T}{\partial x^2}=\frac{\partial}{\partial x}\left(\frac{\partial T}{\partial T^*}\cdot\frac{\partial T^*}{\partial\theta}\cdot\frac{\partial\theta}{\partial x}\right)=\frac{\partial}{\partial\theta}\left(\frac{\partial T}{\partial T^*}\cdot\frac{\partial T^*}{\partial\theta}\cdot\frac{\partial\theta}{\partial x}\right)\frac{\partial\theta}{\partial x}=\frac{(T_w-T_\infty)}{R^2}\frac{\partial^2 T^*}{\partial\theta^2} \qquad 2.56(d)$$

$$\frac{\partial^2 T}{\partial z^2}=\frac{\partial}{\partial z}\left(\frac{\partial T}{\partial T^*}\cdot\frac{\partial T^*}{\partial Z}\cdot\frac{\partial Z}{\partial z}\right)=\frac{\partial}{\partial Z}\left(\frac{\partial T}{\partial T^*}\cdot\frac{\partial T^*}{\partial Z}\cdot\frac{\partial Z}{\partial z}\right)\frac{\partial Z}{\partial z}=\frac{(T_w-T_\infty)}{L_b^2}\frac{\partial^2 T^*}{\partial Z^2} \qquad 2.56(e)$$

$$\frac{\partial u}{\partial y}=\frac{\partial u}{\partial u^*}\cdot\frac{\partial u^*}{\partial y^*}\cdot\frac{\partial y^*}{\partial y}=\frac{U_\infty}{C}\frac{\partial u^*}{\partial y^*} \qquad 2.56(f)$$

$$\frac{\partial w}{\partial y} = \frac{\partial w}{\partial w^*} \cdot \frac{\partial w^*}{\partial y^*} \cdot \frac{\partial y^*}{\partial y} = \frac{U_\infty}{C} \frac{\partial w^*}{\partial y^*}$$

2.56(g)

And by substituting these equations 2.56 (a), (b), (c), (d), (e), (f) and (g) in the specific energy equation, yielded equation 2.57.

$$\rho C_p U_\infty (T_w - T_\infty) \left(\frac{1}{C} \frac{\partial T^*}{\partial t^*} + \frac{u^*}{R} \frac{\partial T^*}{\partial \theta} + \frac{w^*}{L_b} \frac{\partial T^*}{\partial Z} \right) = k(T_w - T_\infty) \left(\frac{1}{R^2} \frac{\partial^2 T^*}{\partial \theta^2} + \frac{1}{L_b^2} \frac{\partial^2 T^*}{\partial Z^2} \right) +$$

$$2\mu \frac{U_\infty^2}{C^2} \left[\left(\frac{\partial u^*}{\partial y^*} \right)^2 + \left(\frac{\partial w^*}{\partial y^*} \right)^2 \right] + \sigma B_0^2 U_\infty^2 \left(u^{*2} + w^{*2} \right)$$

(2.57)

The equation was re-written as in equation 2.58

$$\left(\frac{1}{C} \frac{\partial T^*}{\partial t^*} + \frac{u^*}{R} \frac{\partial T^*}{\partial \theta} + \frac{w^*}{L_b} \frac{\partial T^*}{\partial Z} \right) = \frac{k}{\rho C_p U_\infty} \left(\frac{1}{R^2} \frac{\partial^2 T^*}{\partial \theta^2} + \frac{1}{L_b^2} \frac{\partial^2 T^*}{\partial Z^2} \right) +$$

$$2\mu \frac{U_\infty}{\rho C_p (T_w - T_\infty) C^2} \left[\left(\frac{\partial u^*}{\partial y^*} \right)^2 + \left(\frac{\partial w^*}{\partial y^*} \right)^2 \right] + \frac{\sigma B_0^2 U_\infty}{\rho C_p (T_w - T_\infty)} \left(u^{*2} + w^{*2} \right)$$

(2.58)

The non-dimensionalized energy equation 2.58 contains Prandtl, Eckert and Peclet non-dimensional numbers.

Prandtl Number (Pr)

Prandtl number (Pr) gives the ratio of viscous force to the thermal force and is defined as;

$$\mathrm{Pr} = \frac{C_p \mu}{k} = \frac{\vartheta}{\left(k / \rho C_p \right)}$$

(2.59)

Where $\left(k / \rho C_p \right)$ is the thermal diffusivity and $\vartheta = \frac{\mu}{\rho}$. Fluids that are more viscous have a large

value of ϑ and thus it follows a large Prandtl number. Fluid that are good conductors of heat

have relatively large $\left(k \big/ \rho C_p \right)$ and this occurs in liquid metals whose Prandtl numbers are correspondingly small such as mercury with (Pr=0.023)

Peclet Number (Pe)

If the Prandtl number is divided with $\dfrac{u^2 \mu}{L_b}$, then the non-dimensional number produced is known as the Peclet number which is small when viscous force is small while thermal force is large.

$$Pe = \frac{\rho u L C_p}{k} \tag{2.60}$$

Eckert number (Ec)

The Eckert number (Ec) expresses the relationship between the kinetic energy in the flow and the enthalpy.

It is given as; $\quad Ec = \dfrac{U_\infty^2}{C_p \Delta T}$ \hfill (2.61)

It represents the conversion of kinetic energy into internal energy by the work that is done against the viscous fluid stresses. It have been deduced that a positive Eckert number implies cooling of the stretching sheet (or loss of heat from the sheet to the fluid)

Equation (2.55) and equation (2.58) are then simultaneously solved numerically using finite difference iteration method. The final solution is obtained after successive iterations, beginning with an initial distribution guess of zero values. The results, with no magnetic effects or thermal aspects, have complete agreement with that of Nada and Osman, (2007).

CHAPTER THREE

3.0 THE METHODOLOGY

In this chapter, the method of solution is discussed and the governing equations are presented in their finite difference forms. The final set of the equations are also presented in this chapter and these are the equations that were implemented in a MATLAB version 7.14.0.739 computer program.

3.1 FINITE DIFFERENCE TECHNIQUE

The finite difference approximations for derivatives are one of the simplest methods to solve differential equations. The principle of finite difference methods is close to the numerical schemes used to solve ordinary and partial differential equations. It consists in approximating the differential operator by replacing the derivatives in the equation using difference quotients. The domain is partitioned in space and in time and approximations of the solution are computed at the space or time points. Equations (2.55) and (2.58) are non-linear hence cannot be solved analytically. Therefore the finite difference method was used in their solution subject to the initial conditions

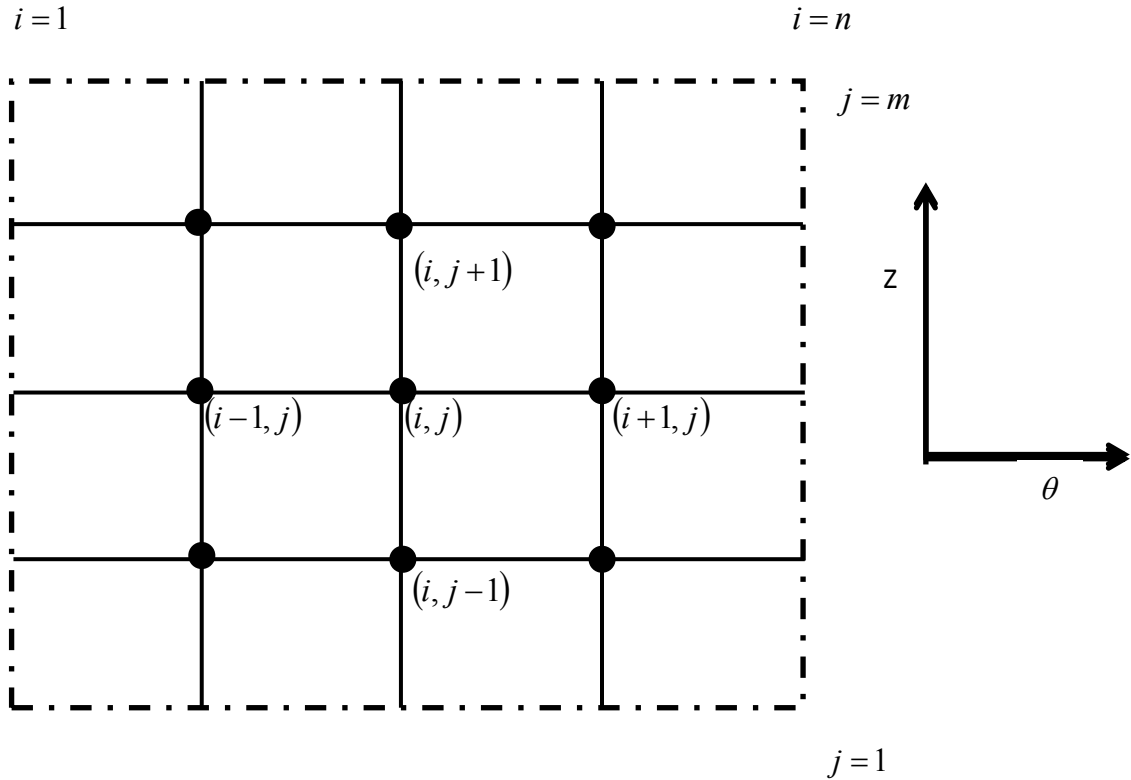### 3.1.1   The Reynolds Equation in Finite difference

Consider the specific non-dimensional Reynolds equation (2.55), the bearing geometry and the magnetic field model. The film thickness H depends totally on the change of the angle θ and hence the derivatives of H with respect to θ remains while those of Hm with respect to θ vanishes, also the derivatives of H with respect to Z disappears while those of Hm with respect to Z remain thus the equation reduces to equation 3.1;

$$3H^2 \frac{\partial H}{\partial \theta} \cdot \frac{\partial P^*}{\partial \theta} + H^3 \frac{\partial^2 P^*}{\partial \theta^2} + \frac{1}{4\beta^2} H^3 \frac{\partial^2 P^*}{\partial Z^2} = 6 \frac{\partial H}{\partial \theta} + +\alpha \left\{ H^3 \left(\frac{\partial H_m}{\partial z} \right)^2 + H^3 H_m \frac{\partial^2 H_m}{\partial z^2} \right\} \qquad (3.1)$$

And applying the finite difference technique, using the central difference method, the first and

second derivatives reduce to equations 3.2(a) and 3.2(b);

$$\frac{\partial P^*}{\partial \theta} = \frac{P^*_{(i+1,j)} - P^*_{(i-1,j)}}{2\Delta\theta} \qquad\qquad \frac{\partial^2 P^*}{\partial \theta^2} = \frac{P^*_{(i+1,j)} + P^*_{(i-1,j)} - 2P^*_{(i.j)}}{(\Delta\theta)^2} \qquad 3.2(a)$$

$$\frac{\partial P^*}{\partial Z} = \frac{P^*_{(i,j+1)} - P^*_{(i,j-1)}}{2\Delta Z} \qquad\qquad \frac{\partial^2 P^*}{\partial Z^2} = \frac{P^*_{(i,j+1)} + P^*_{(i,j-1)} - 2P^*_{(i.j)}}{(\Delta Z)^2} \qquad 3.2(b)$$

Figure 3.1: Finite difference mesh

After using the central difference technique, the Reynolds equation reduces to equation 3.3;

$$P_{i,j}^{*}\left[\frac{2\left(H_{i,j}\right)^{3}}{\left(\Delta\theta\right)^{2}}+\frac{1}{2\beta^{2}}\frac{\left(H_{i,j}\right)^{3}}{\left(\Delta Z\right)^{2}}\right]=-3\left(H_{i,j}\right)^{2}\left[\frac{H_{i+1,j}-H_{i-1,j}}{2\Delta\theta}\right]\left[\frac{P_{i+1,j}-P_{i-1,j}}{2\Delta\theta}\right]-\left(H_{i,j}\right)^{3}\left[\frac{P_{i+1,j}-P_{i-1,j}}{\left(\Delta\theta\right)^{2}}\right]$$

$$-\frac{\left(H_{i,j}\right)^{3}}{4\beta^{2}}\left[\frac{P_{i,j+1}-P_{i,j-1}}{\left(\Delta Z\right)^{2}}\right]+3\left[\frac{H_{i+1,j}-H_{i-1,j}}{\Delta\theta}\right]+\alpha\left(H_{i,j}\right)^{3}\left\{\left(\frac{Hm_{i,j+1}-Hm_{i,j-1}}{2\Delta Z}\right)^{2}+Hm_{i,j}\left(\frac{Hm_{i,j+1}-Hm_{i,j-1}+2Hm_{i,j}}{\left(\Delta Z\right)^{2}}\right)\right\}$$

$$(3.3)$$

3.1.2 The Energy Equation in Finite difference

And applying the finite difference technique to the specific non-dimensional energy equation 2.58, and using the central difference method, the first and second derivatives yielded equation 3.4(a) and equations 3.4(b) respectively;

$$\frac{\partial T^{*}}{\partial\theta}=\frac{T_{(i+1,j)}^{*}-T_{(i-1,j)}^{*}}{2\Delta\theta} \qquad \frac{\partial^{2}T^{*}}{\partial\theta^{2}}=\frac{T_{(i+1,j)}^{*}+T_{(i-1,j)}^{*}-2T_{(i.j)}^{*}}{\left(\Delta\theta\right)^{2}} \qquad 3.4(a)$$

$$\frac{\partial T^{*}}{\partial Z}=\frac{T_{(i,j+1)}^{*}-T_{(i,j-1)}^{*}}{2\Delta Z} \qquad \frac{\partial^{2}T^{*}}{\partial Z^{2}}=\frac{T_{(i,j+1)}^{*}+T_{(i,j-1)}^{*}-2T_{(i.j)}^{*}}{\left(\Delta Z\right)^{2}} \qquad 3.4(b)$$

After using the central difference technique, the energy equation was written as equation 3.5;

$$\frac{u^{*}}{R}\frac{T_{(i+1,j)}^{*}-T_{(i-1,j)}^{*}}{2\Delta\theta}+\frac{w^{*}}{L_{b}}\frac{T_{(i,j+1)}^{*}-T_{(i,j-1)}^{*}}{2\Delta Z}=\frac{K}{\rho C_{p}U_{\infty}}\left[\frac{1}{R^{2}}\frac{T_{(i+1,j)}^{*}+T_{(i-1,j)}^{*}-2T_{(i.j)}^{*}}{\left(\Delta\theta\right)^{2}}+\frac{1}{L_{b}^{2}}\frac{T_{(i,j+1)}^{*}+T_{(i,j-1)}^{*}-2T_{(i.j)}^{*}}{\left(\Delta Z\right)^{2}}\right]$$

$$+2\mu^{*}\frac{U_{\infty}}{\rho C_{p}\left(T_{w}-T_{\infty}\right)C^{2}}\left[\left(\frac{\partial u^{*}}{\partial y^{*}}\right)^{2}+\left(\frac{\partial w^{*}}{\partial y^{*}}\right)^{2}\right]+\frac{\sigma\beta_{0}^{2}U_{\infty}}{\rho C_{p}\left(T_{w}-T_{\infty}\right)}\left(u^{*2}+w^{*2}\right) \qquad (3.5)$$

Equation 3.5 was re-written as equation 3.6

$$\frac{K}{\rho C_p U_\infty}\left\{\frac{2T^*_{(i,j)}\left[L_b^2(\Delta Z)^2 + R^2(\Delta\theta)^2\right]}{R^2 L_b^2(\Delta\theta)^2(\Delta Z)^2}\right\} = \frac{K}{\rho C_p U_\infty}\left\{\frac{L_b^2(\Delta Z)^2\left(T^*_{(i+1,j)} + T^*_{(i-1,j)}\right) + R^2(\Delta\theta)^2\left(T^*_{(i,j+1)} + T^*_{(i,j-1)}\right)}{R^2 L_b^2(\Delta\theta)^2(\Delta Z)^2}\right\}$$

$$-\left[\frac{L_b(\Delta Z)u^*\left(T^*_{(i+1,j)} - T^*_{(i-1,j)}\right) + R(\Delta\theta)w^*\left(T^*_{(i,j+1)} - T^*_{(i,j-1)}\right)}{2RL_b(\Delta\theta)(\Delta Z)}\right] + 2\mu^*\frac{U_\infty}{\rho C_p(T_w - T_\infty)C^2}\left[\left(\frac{\partial u^*}{\partial y^*}\right)^2 + \left(\frac{\partial w^*}{\partial y^*}\right)^2\right]$$

$$+\frac{\sigma\beta_0^2 U_\infty}{\rho C_p(T_w - T_\infty)}\left(u^{*2} + w^{*2}\right) \tag{3.6}$$

And making $T^*_{i,j}$ the subject of equation 3.6 yielded equation 3.7;

$$2T^*_{(i,j)} = \left\{\frac{L_b^2(\Delta Z)^2\left(T^*_{(i+1,j)} + T^*_{(i-1,j)}\right) + R^2(\Delta\theta)^2\left(T^*_{(i,j+1)} + T^*_{(i,j-1)}\right)}{L_b^2(\Delta Z)^2 + R^2(\Delta\theta)^2}\right\}$$

$$-\left(\frac{\rho C_p U_\infty}{K}\right)\frac{RL_b(\Delta\theta)(\Delta Z)}{L_b^2(\Delta Z)^2 + R^2(\Delta\theta)^2}\left[\frac{L_b(\Delta Z)u^*\left(T^*_{(i+1,j)} - T^*_{(i-1,j)}\right) + R(\Delta\theta)w^*\left(T^*_{(i,j+1)} - T^*_{(i,j-1)}\right)}{2}\right]$$

$$+\left(\frac{R^2 L_b^2(\Delta\theta)^2(\Delta Z)^2}{L_b^2(\Delta Z)^2 + R^2(\Delta\theta)^2}\right)\left[2\mu^*\frac{U_\infty^2}{K(T_w - T_\infty)C^2}\left[\left(\frac{\partial u^*}{\partial y^*}\right)^2 + \left(\frac{\partial w^*}{\partial y^*}\right)^2\right] + \frac{\sigma\beta_0^2 U_\infty^2}{K(T_w - T_\infty)}\left(u^{*2} + w^{*2}\right)\right] \tag{3.7}$$

The equations (3.3) and (3.7) are the final set of equations and were solved simultaneously using

a computer code in MATLAB application software version 7.14.0.739.

4.0   RESULTS AND DISCUSSIONS

Equations (3.4) and (3.9) were solved using the MATLAB version 7.14.0.739 computer code in Appendix I. The pressure and the temperature distributions are discussed in this chapter while other parameters such as magnetic coefficient, couple force parameter and eccentricity ratio are being varied. The figures produced as per the code in Appendix I are thus discussed below;

4.1 PRESSURE DISTRIBUTIONS
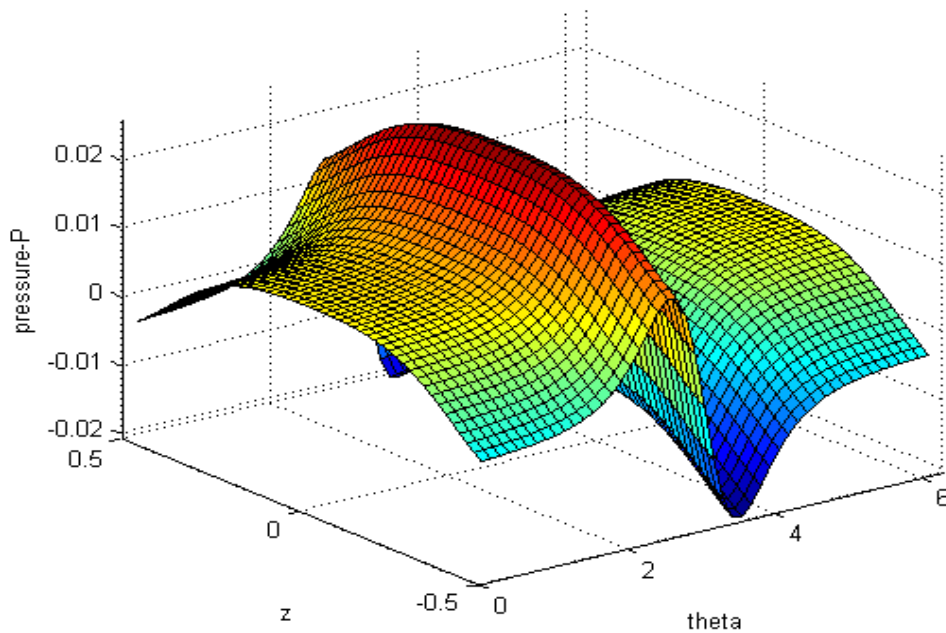
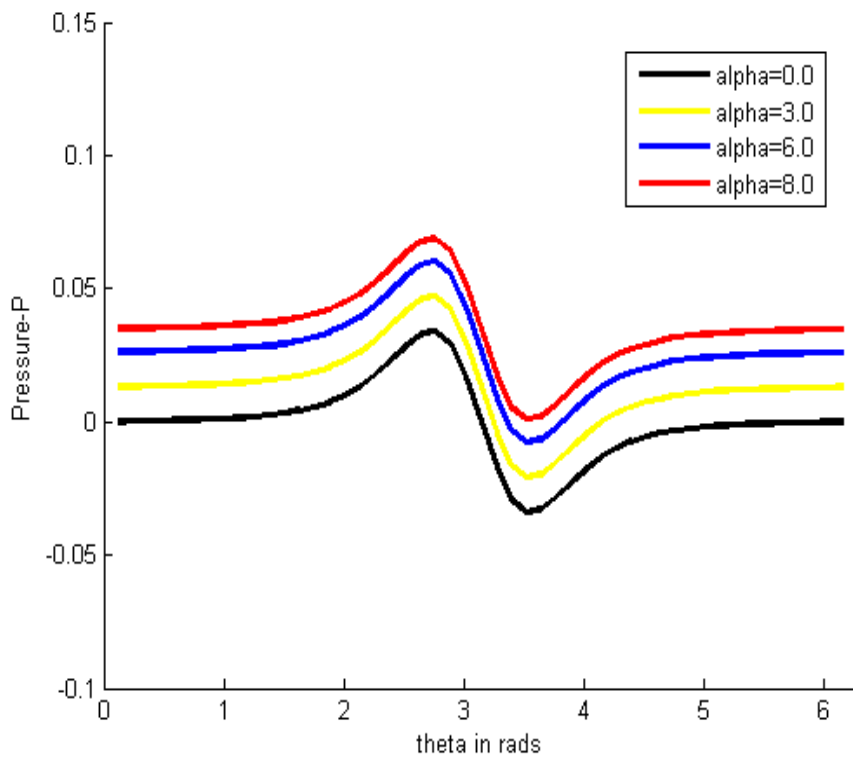**Figure 4.1: Plot surface of pressure with theta and z**

The results have been worked out for ferro-fluids with couple stresses assuming constant viscosity coefficient and density of the lubricant. The result as in Figure 4.1 gives the

dimensionless pressure distribution in circumferential and axial directions with eccentricity ratio for different values of the couple stress parameter. It represents a surface of pressure against both circumferential and axial directions. The results were obtained for constant eccentricity ratio e, length to diameter ratio β of 1.0 and varied couple stress parameter L of 0.0, 0.2 and 0.4 and comparing this results with (Abdo, 2009) where L = 0.0 is the Newtonian lubricant case they have good correlation since the trend is similar. The results are also determined for magnetic coefficient α = 0.0 which is the non-magnetic lubricant case and α = 2.0 to 8.0 the magnetic lubricant case and comparing with (Nada and Osman, 2007) again we find that there is good correlation. The pressure distribution in the circumferential direction at the bearing mid-plane (bearing centerline) for different values of couple stress parameter and a constant value of magnetic coefficient are shown in Figure 4.2 for eccentricity ratio e = 0.6.
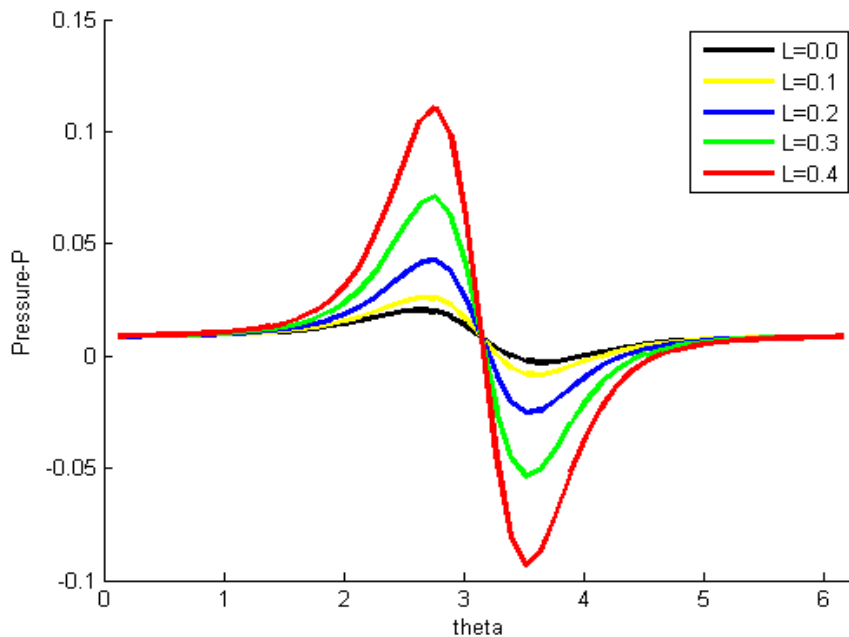
Figure 4.2: Plot of pressure against theta with increasing couple stress

The results in Figure 4.2 for the case of magnetic lubricant, there is an increase of the absolute pressure with increasing value of couple stress parameter L, at a constant eccentricity ratio used. This increase is more pronounced as we increase the value of the couple stress parameter. Thus, the absolute pressure is increasing as the value of the couple stress parameter increases. From the basic definition of pressure where it is given as force per unit surface area, therefore, the couple stress is as force being added in the fluid surface while the bearing surface remains a constant. Hence the increase in pressure is due to the increase in the couple stress.

Figure 4.3: Plot surface of pressure against theta with varied magnetic coefficient

Considering the magnetic effect, where the value of the magnetic coefficient is varied to see its effect on the absolute pressure. This is observed as from Figure 4.3. There is a large increase of the pressure as the value of the magnetic coefficient increases. The maximum pressure is shifted

to the angle $\theta = 0.5\pi$. Due to symmetry from Figure 4.1 it is clear that the pressure increases in magnitude in the negative way after another 0.5π mark angle. Effect of alpha is also determined at a constant value of the eccentricity ratio. At this value of eccentricity ratio, there are two maximum pressure points as shown in Figure 4.1 and also according to Abdo, 2009. The first at $\theta = 0.5\pi$ due to the magnetic effect and value of the couple stress parameter L and the other at nearly $\theta = \pi$ due to the hydrodynamic effect, its value depends mainly on the couple stress parameter L.
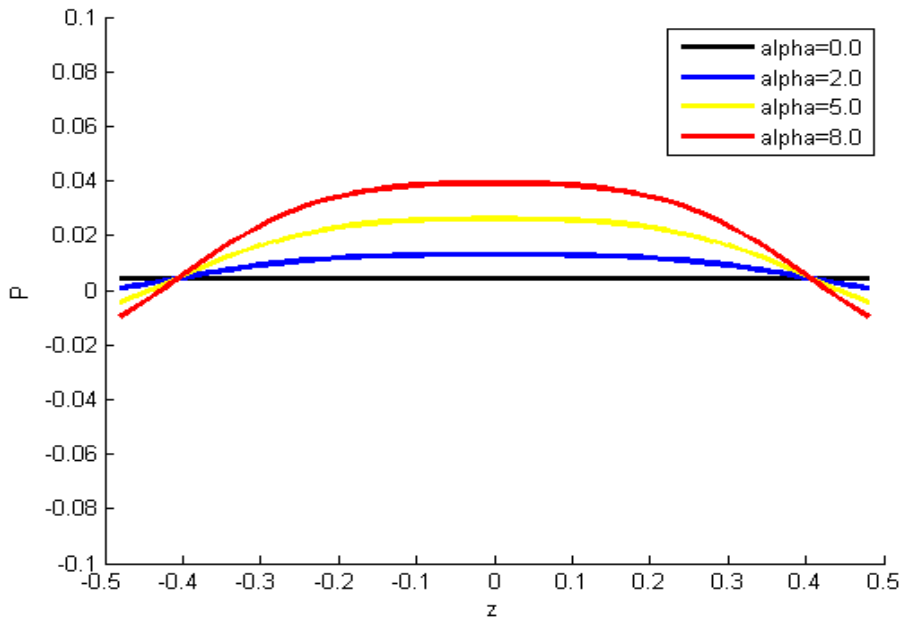

Figure 4.4: Plot surface of pressure with theta and z

Figure 4.4 represents the plot of pressure against the length of the bearing for different magnetic coefficient for couple stress parameter ($L = 0.2$). The result from the graph shows that as we increase the value of the magnetic coefficient the pressure also increases. The magnetic contribution is more along the length of the bearing and it is highest at the middle of the bearing as evident in Figure 4.4. Some symmetry is seen at the center of the bearing that is at $Z = 0.0$. All

this is being analyzed considering the eccentricity ratio being held a constant. It can also be seen that the pressure of the bearing lubricated with couple stress fluid increases with increasing couple stress parameter. Bearings pressure with magnetic lubricant and couple stress are greater than that with nonmagnetic lubricant and without the couple stress. This is due to the fact that force is increased due to couple force while the surface area to which the force acts on remains a constant.
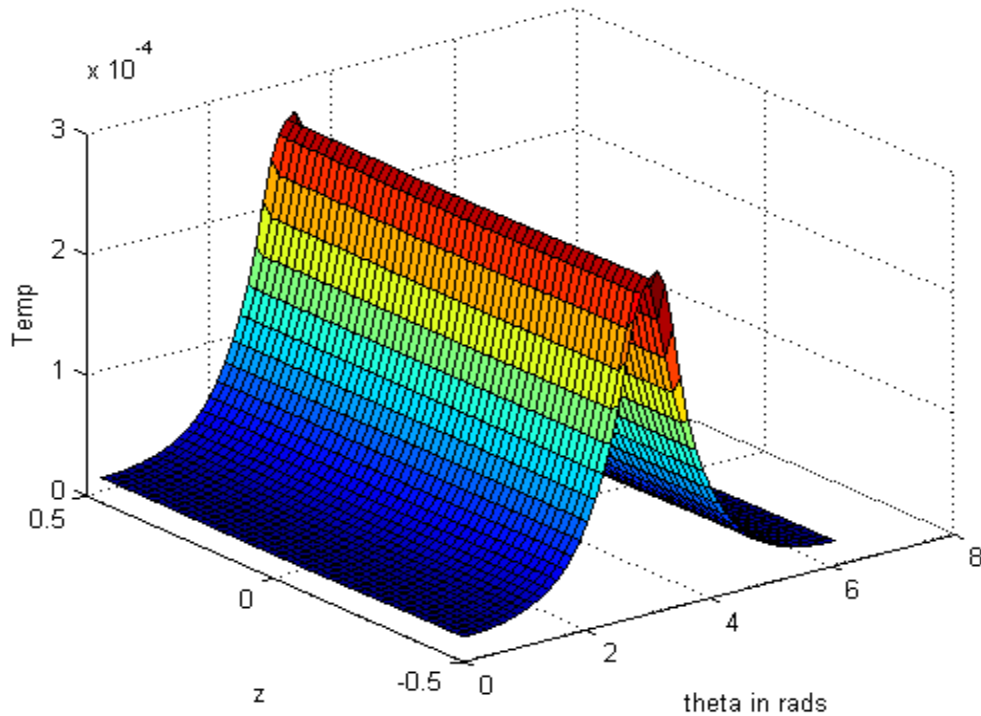
4.2 TEMPERATURE DISTRIBUTIONS AND VELOCITY PROFILES
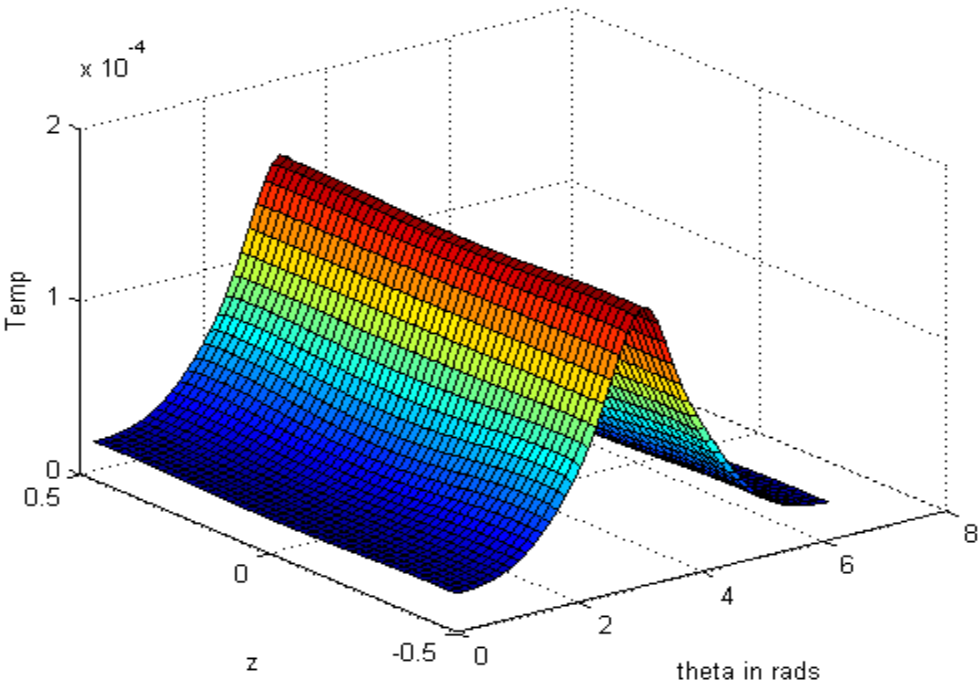
Figure 4.5: Plot of surface of temperature with theta and z at $L = 0.2$

Figure 4.5 shows the Non-dimensional temperature distribution (T) for constant eccentricity ratio applying some magnetic force and for length to diameter ratio 1.0 across the bearing ends. This figure displays temperature distributions over the whole bearing at the same eccentricity ratio applying magnetic force, $\alpha = 0.8$ and the couple stress parameter $L = 0.2$. The surface as seen in

the figure 4.5 clearly shows the temperature distributions with the bearing length and theta θ. It is found that the temperature increases slightly in the region $\theta = 0.0$ to $\theta = 0.5\pi$ after that the rate increases rapidly within the region $\theta = 0.5\pi$ to $\theta = 1.5\pi$, then rate of increase of temperature in the region $\theta = 1.5\pi$ to $\theta = 2\pi$ is approximately considered to be dropping as the fluid goes back to meet with fresh lubricant at insertion point at $\theta = 0.0$. Due to no slip property, lubricant layers slid over each other and thus due to friction the temperature increases

Figure 4.6: Plot of surface of temperature with theta and z at $L = 0.5$

Temperature profile again is shown clearly in the wire frame Figure 4.6 it shows the 3D Temperature distributions over the whole bearing at the same eccentricity ratio after applying magnetic force, $\alpha = 0.8$ and the couple stress parameter $L = 0.5$. It is evident that as the value of couple stress parameter increases, the temperature of the bearing increases as well. This is seen as we compare the non-dimensional maximum temperatures in Figure 4.5 which is

41

approximately 1.5 and that in Figure 4.6 which is approximately 2.5. Therefore, the higher the couple stress parameter L increases so does the bearing temperature.
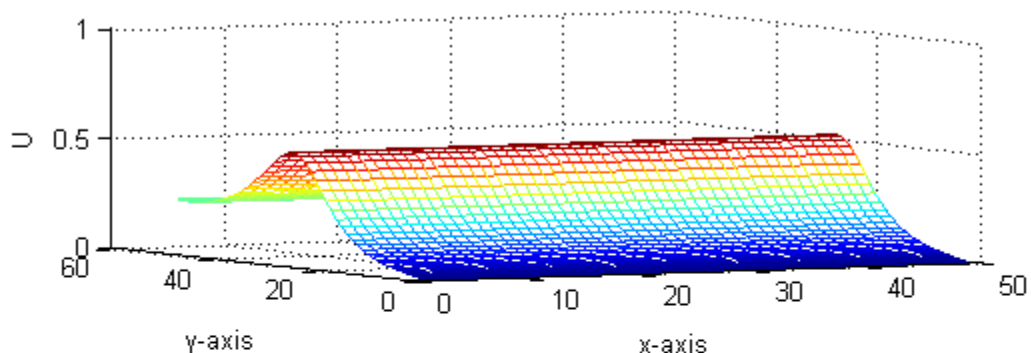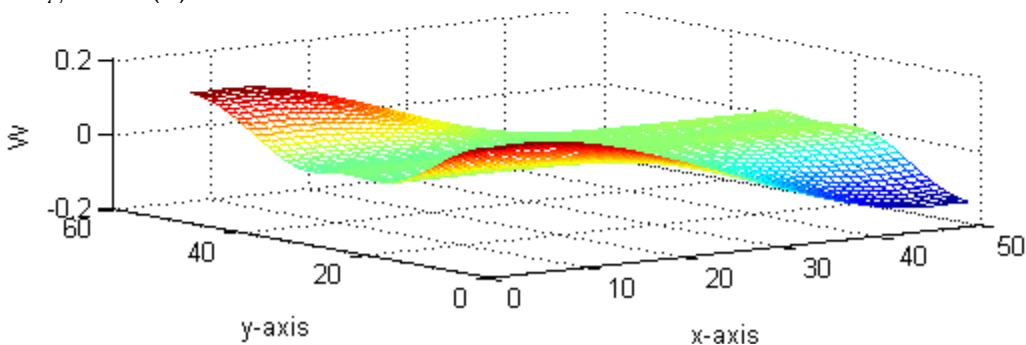

Figure 4.7(a)

Figure 4.7(b)

Figure 4.7: Velocity profiles in both circumferential and axial directions respectively

From Figure 4.7(a), we observe that the non-dimensional velocity increases with decrease in the film thickness which is in the circumferential direction. This velocity is highest at the lowest value of the film thickness where the bearing pressure is highest. The film thickness is affected by the amount of force applied on the bearing thus the appearance of the eccentricity ratio. In the bulk of the liquid, each molecule is pulled equally in every direction by neighboring liquid molecules, resulting in a net force of zero. Therefore, the force applied to this fluid is the load being carried by the bearing.

Velocity along the axial direction is as in Figure 4.7(b). This velocity is unstable due to the position of the groove. Having that the groove is at some specific position, the lubricant as it enters the bearing, it takes the velocity of the journal due to no slip condition. Along the bearing therefore, the velocity is varied until at some position away from the groove where this velocity is approximately a constant.
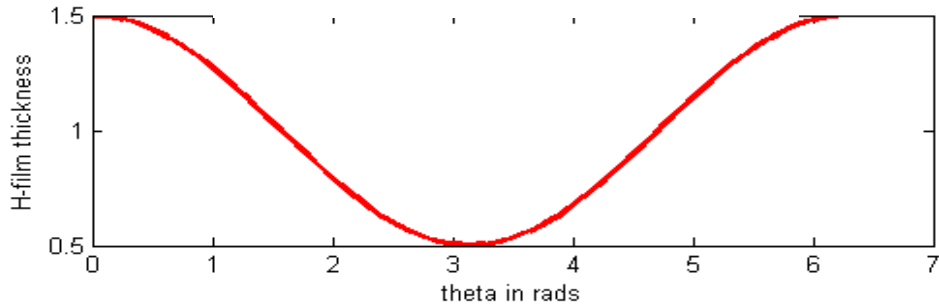

Figure 4.8(a)
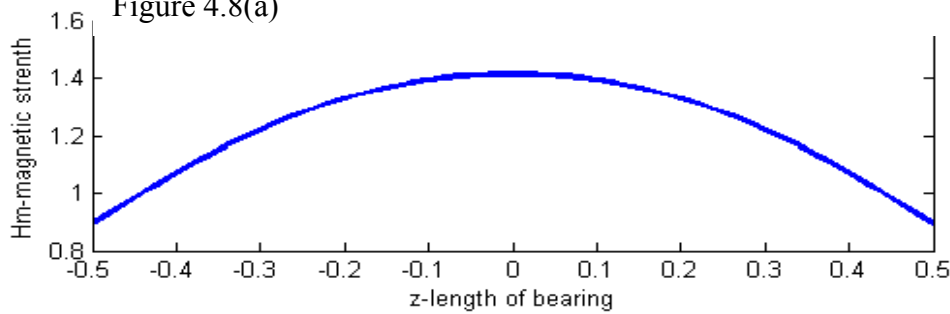
Figure 4.8(b)

Figure 4.8: Plot of film thickness vs. theta and magnetic strength vs. bearing length

Figure 4.8 a) represents the plot of film thickness against the arc length θ. The film thickness reduces from some value at $\theta = 0.0$ to $\theta = \pi$ and then increases back to the same value at the point of lubricant admission. This is due to the geometry of the bearing as schemed in the Figure 1.3 which results to the non-dimensional film thickness being given as in equation (3.56). Considering the boundary conditions and the geometry, it is clear that the pressure and the temperature are symmetrical about the middle plane of the bearing $(Z = 0)$.

Figure 4.8 b) represents the plot of magnetic strength applied against the length of the bearing Z. The curve shows that the magnetic strength increases from $(Z = -0.5)$ to $(Z = 0)$ where it starts again to reduce back to the initial value at $(Z = 0.5)$. This is similar to the results of Abdo, 2009 where a concentric finite wire was placed at the center of the shaft and some current passed through to produce the magnetic strength. Therefore, induced magnetic field is produce by the effect of the current passing through the wire according to Maxwell's equations and this force is as in the equation (2.51).
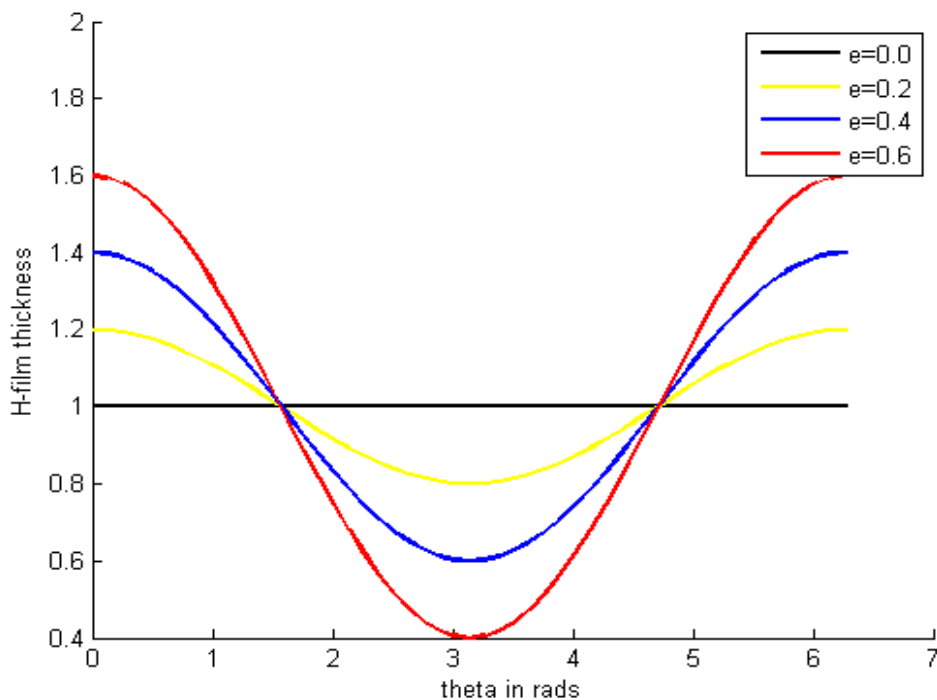
Figure 4.9: Graph of film thickness against theta at different eccentricity ratio values

Figure 4.9 represents the plot of film thickness against arc length θ with eccentricity ratio ranging from $e = 0.0$ to $e = 0.6$. It is found that as the eccentricity ratio increases so does the film thickness. This effect increases the hydrodynamic effect hence the bearing can carry higher values of the load applied on the bearing. Also the temperature distribution is affected by

changing the eccentricity ratio; higher eccentricities are always associated with higher temperature rise. This agrees with that of Monira, 1982. The results indicate that the magnetic lubrication has insignificant effect on the lubricant maximum temperature at all eccentricity ratio. In fact, it is from the good benefit for the magnetic lubricant.

CHAPTER FIVE

5.0 CONCLUSIONS AND RECOMMENDATIONS

5.1 CONCLUSIONS

The performance finite elasto-hydrodynamic journal bearing lubricated with ferrofluid and with couple stresses have been investigated. The conclusions that have been arrived at and the contributions added are, herein, presented:

1. Under magnetic lubricant, the results concluded that the magnetic lubrication gives higher pressure distribution. This would therefore lead to increased load carrying capacity.

2. For the magnetic lubrication, the increase of the pressure is not accompanied by increase of the friction losses. For constant loads, decrease of the operating eccentricity ratio (compared to conventional lubricated bearing) may lead to decrease of the frictional forces.

3. The bearing performance is modified when the magnetic effects are comparable with the elasto-hydrodynamic ones, namely; when the bearing operates at low eccentricity ratios (e) and high values of (α), this requires that the magnetic field to be high, the rotation speed is low and the relative clearance is large. Far from such conditions the elasto-hydrodynamic effects prevail considerably and insignificant effect for the magnetic lubrication is obtained.

4. For journal bearing lubricated by magnetic fluids with couple stresses both the pressure and load carrying capacity increase with the increase of the couple stress parameter (L). The increase is more pronounced for bearings operating at higher values of eccentricity

ratios. The attitude angle decreases with increasing the couple stress parameter especially at high values of eccentricity ratio this influence qualitatively agrees with some previous works.

5. Temperature of the bearing increases due to the friction between the layers of the fluid. The temperature is absorbed by the magnetic particles in the fluid thus maintaining moderate temperature in the bearing. The couple stresses are observed to increase the temperature of the bearing. Considering the effect of joules heating in the bearing, it was observed that joules heating effects are minute and thus negligible.

It could be concluded from the above that fluids with microstructure (couple stress) are better lubricants than Newtonian fluids especially if they were prepared to become magnetic fluids. The results provide to engineers useful information to design machine elements and bearing systems with a higher life expectancy and efficiency.

5.2   RECOMMENDATIONS

In this study, we have considered that the fluid is incompressible in that the density is held constant and that the viscosity coefficient is also constant. From the study, having that there is change in temperature, then the viscosity and density of the fluid is changing as well. We therefore recommend that an extension in research of the same elasto-hydrodynamic journal bearing with viscosity and the density being taken as variable be a food for thought for advanced research in this area.

The bearing studied was considered to work under perfect condition and therefore we recommend that if it could have a broken part or a hole and more lubricant is lost, a study should be done to facilitate how such a condition could be managed. We also recommend that a study be done on a combination of a journal bearing and other bearing, to observe whether such combinations would be applicable to improving the bearing performance and efficiency.

REFERENCES

Ariman, T, M A Turk, and N D Sylvester. (1973) "Microcontinuum fluid mechanics-a review." 905-930. International Journal of Engineering Science.

Ariman, T; Turk, M A; Sylvester, N D. (1974). "Applications of microcontinuum fluid mechanics." 273-293. International Journal of Engineering Science.

Abdo S. H., Osman S. G., Nada G. G. and Abdel-Jaber T. G. (2009). Thermal Effects on Hydrodynamic Journal Bearings Lubricated by magnetic Fluids with Couple Stresses. Thesis in Mechanical Design and Production Engineering. Cairo University.

Booker, J F, and K H Huebner. (1972). "Application of finite elements to lubrication: An engineering approach." Journal of lubrication technology.

Bujurke, N M, and N B Naduvinamani. (1990). "The lubrication of lightly loaded cylinders in combined rolling, sliding and normal with couple stress fluid." International Journal of Mechanical Sciences.

Chum, S M. (2004). "Thermohydrodynamic lubriction analysis of high speed journal bearing considering variable density and variable specific heat." Tribology International.

Cowley, M D, and R E Rosensweig. (1967). "The interfacial stability of ferromagnetic fluid." Journal of Fluid Mechanics.

Cavalca K. L. and Daniel G. B., (2013). "Evaluation of the thermal effects in tilting pad bearing" Scientific world Journal.

Govindaraj R., and Satishkumar V. M. (2012), Design of journal bearing test rig. Sweden: Blekinge Tekniska Hogskola.

Hamrock, B J. (1994). Fundamentals of fluid film lubrication. New York: New York: McGraw-Hill.

Minhui He., Hunter C. and Byrne J. (2005). "Fundamentals of fluid film Journal bearing operstion and modeling," proceeding of the Thirty Fourth Turbo machinery.

Mokhiamer, U M, W A Crosby, and H A El-Gamal. (1999). "A study of a journal bearing lubriacted by fluids with couple stress considering the elasticity of the liner." 194-201. Wear.

Mukesh S., Ashish K. G. and Ashish D. (2012). "Thermo-hydrodynamic analysis of a Journal bearing using CFD as a Tool" International Journal of Science and Research.

Moskowitz, R. (1975). "Designing with ferrofluids" Mechanical Engineering, February, Vol. 97, P. 30-36.

Monira, A. M. (1982). "The Effect of Thermal Aspects on the Performance of Hydrodynamically Lubricated Journal Bearings." Master Thesis in Mechanical Engineering, Faculty of Engineering, Cairo University.

Nada, G S, and T A Osman. (2007). "Static Performance of Finite Hydrodynamic Journal Bearings Lubricated by Magnetic Fluids with Couple Stresses." Egypt: Springer Science and Business Media.

Naduvinamani, N B, P S Hiremath, and G Gurubasavaraj. (2002). "Effect of surface roughness on the static characteristics of rotor bearings with couple stress fluids." 1243-1253. Comput. Struct. 80.

Naduvinamani, N B, P S Hiremath, and G Gurubasavaraj. (2002). "Surface roughness effects in a short porus journal bearing with a couple stress fluid." 333-354. Fluid Mechanics.

Nessil A., Salati L., Hacene B. and Muamar M. (2012). "Journal bearing lubrication Aspect Analysis Using Non-Newtonian Fluids." Scientific World Journal.

Norman O. F., (1995). "A Thermo-elasto-hydrodynamic study of Journal bearings" PhD thesis in Mechanical engineering, University of Wollongong.

Osman, T A. (1999). "Static characteristics of hydrodynamic magnetic bearings working by non-Newtonian Ferro-fluid." 521-536. Cairo: Journal of Engineering and Applied Sci.

Osman T. A., Nada G. S., and Safar Z. S. (2002), *Dynamic characteristics of magnetized journal bearings lubricated with Newtonian and non-Newtonian Ferro-fluids*:Proceedings of sixth international conference on production engineering and design for development, Cairo, Egypt.

Osman, T A, G S Nada, and Z S Safar. (2003). "Different magnetic models in the design of hydrodynamic journal bearings lubricated with non-Newtonian Ferro-fluid." *Tribol. Lett*: 211-223.

Priyanka T. and Veerendra K. (2012). "Analysis of Hydrodynamic Journal bearing- A review" International Journal of Engineering Research and Technology.

Raj, K, and R J Boulton. (1987). "Ferro-fluids-Properties and applications." 233-236. Journal of Material Design.

Rosensweig, R E, R Kaiser, and G Miskolezy. (1969). "Viscosity of magnetic fluid in a magnetic field." Journal of Colloid and Interface Science.

Rosensweing, R E. (1982). "Magnetic fluids." 124-132. Scientific American.

Saynatjoki, M, and K Holmberg. (1982). *Magnetic fluids in sealing and lubrication–a state of art review.* Finland: Technical Research Center of Finland.

Senthil, M Kumar, P R Thyla, and E Anbarasu. (2010). "Numerical analysis of hydrodynamic journal bearing under transient dynamic conditions." *ISSN 1392 – 1207.* Mechanika.

Stokes, V K. (1966). "Couple stresses in fluids." 1709-1715. Physics. Fluids 9.

Zelazo, R E, and J R Melcher. (1969). "Dynamic stability of Ferro-fluids: surface interaction." 1-24. J. Fluid Mechanics.

APPENDICES

APPENDIX 1: COMPUTER CODE IN MATLAB

In order to solve the governing equations (3.3) and (3.7), the following computer program code was developed using MATLAB software version 7.14.0.739, subject to the boundary conditions as discussed herein. The results were obtained by varying various flow parameters, notably couple stress parameter, magnetic coefficient and eccentricity ratio.

```
% NUMERICAL SOLUTION OF JOURNAL BEARING
function kihugaCode3latest()
clear all;
clc;
N=51;
xlower=0;xupper=2*pi;
dx=(xupper-xlower)/(N-1);
x=xlower:dx:xupper;
K=51;
zlower=-.5;zupper=.5;
dz=(zupper-zlower)/(K-1);
z=zlower:dz:zupper;
[h hm g]=coeff3(x,z);
M=51;
ylower=0;yupper=h;
dy=(yupper-ylower)/(M-1);
y=ylower:dy:yupper;
miu=1.5;
p=zeros(N,K);T=zeros(N,M,K);
%%%START=====BOUNDARY CONDITIONS=========%%%%%%%%%%
for i=1:N
    for k=1:K
    p(1,k)=0;
    p(i,1)=0;
    p(N,k)=0;
    p(i,K)=0;
    end
end
Tw=40;Tinf=70;
for i=1:N
    for k=1:K
    for j=1:M
    T(i,1,j)=0;
    T(i,K,j)=0;
    T(i,k,1)=Tinf;
    T(i,k,M)=Tw;
    T(1,k,j)=0;
    T(N,k,j)=0;
    end
    end
```

```matlab
end
%%%END=====BOUNDARY CONDITIONS=========%%%%%%%%%


matrix=ones(N,K);
%% START EXTENDING FXNS h and hm INTO MATRICES%%
hmatrix=zeros(N,K);gmatrix=zeros(N,K);hmmatrix=zeros(N,K);
for i=1:N
    for k=1:K
        hmatrix(i,k)=h(i)*matrix(i,k);
        gmatrix(i,k)=g(i)*matrix(i,k);
        hmmatrix(i,k)=hm(k)*matrix(i,k);
    end
end

Hc=hmatrix(2:N-1,2:K-1);Hxr=hmatrix(3:N,2:K-1);Hxl=hmatrix(1:N-2,2:K-1);% extended to matrix form
Gc=gmatrix(2:N-1,2:K-1);Gxr=gmatrix(3:N,2:K-1);Gxl=gmatrix(1:N-2,2:K-1);
Hmc=hmmatrix(2:N-1,2:K-1); Hmzu=hmmatrix(2:N-1,3:K); Hmzd=hmmatrix(2:N-1,1:K-2);
Pc=p(2:N-1,2:K-1);Pxr=p(3:N,2:K-1);Pxl=p(1:N-2,2:K-1); Pzu=p(2:N-1,3:K);Pzd=p(2:N-1,1:K-2);

[A0 A1 A2 A3 A4]=coeff1(Hc,Hxr,Hxl,Gc,Gxr,Gxl,Hmc,Hmzu,Hmzd,Pxr,Pxl,Pzu,Pzd,dx,dz);
p=(A1./(eps+A0))+(A2./(eps+A0))-(A3./(eps+A0))-(A4./(eps+A0));

%% END EXTENDING FXNS h and hm INTO 3x3 MATRICES%%
matrixY=ones(N,K,M);y3D=zeros(N,K,M);h3D=zeros(N,K,M);
hm3D=zeros(N,K,M);p3D=zeros(N,K,M);p2=zeros(N,K,M);
p2(2:N-1,2:K-1)=p;
for i=1:N
    for k=1:K
        for j=1:M
            y3D(i,k,j)=y(j)*matrixY(i,k,j);
            h3D(i,k,j)=h(i)*matrixY(i,k,j);
            hm3D(i,k,j)=hm(k)*matrixY(i,k,j);
            p3D(i,k,j)=p2(i,k)*matrixY(i,k,j);
        end
    end
end
ys=size(y3D);
Y3D=y3D(2:N-1,2:K-1,2:M-1);H3D=h3D(2:N-1,2:K-1,2:M-1);Hm3D=hm3D(2:N-1,2:K-1,2:M-1);
Hmzu3D=hm3D(2:N-1,3:K,2:M-1); Hmzd3D=hm3D(2:N-1,1:K-2,2:M-1);
Pxr3D=p3D(3:N,2:K-1,2:M-1);Pxl3D=p3D(1:N-2,2:K-1,2:M-1); Pzu3D=p3D(2:N-1,3:K,2:M-1);
Pzd3D=p3D(2:N-1,1:K-2,2:M-1);

[u w]=coeff(Y3D,H3D,miu,Hm3D,Hmzu3D,Hmzd3D,Pxr3D,Pxl3D,Pzu3D,Pzd3D,dx,dz);
vel=size(u);
%% START EXTENDING FXNS u and w TO SAME DIMENSIONS AS T(X,Y,Z) %%
u2=zeros(N,K,M);w2=zeros(N,K,M);
u2(2:N-1,2:K-1,2:M-1)=u;
w2(2:N-1,2:K-1,2:M-1)=w;

%% END EXTENDING FXNS u and w TO SAME DIMENSIONS AS T(X,Y,Z) %%
uC=u2(2:N-1,2:K-1,2:M-1);uyR=u2(2:N-1,2:K-1,3:M);uyL=u2(2:N-1,2:K-1,1:M-2);
wC=w2(2:N-1,2:K-1,2:M-1);wyR=w2(2:N-1,2:K-1,3:M);wyL=w2(2:N-1,2:K-1,1:M-2);
Tzu=T(2:N-1,3:K,2:M-1);Tzd=T(2:N-1,1:K-2,2:M-1);Txr=T(3:N,2:K-1,2:M-1);Txl=T(1:N-2,2:K-1,2:M-1);

[Tpat5 Tpat6 Tpat7 Tpat8 Tpat9]=temp(dx,dy,dz,miu,Tzu,Tzd,Txr,Txl,uyR,uyL,wyR,wyL,uC,wC);
```

```
T=Tpat5-Tpat6+Tpat7*(Tpat8+Tpat9);

figure(1)
surf(x(2:N-1),z(2:K-1),p')
figure(2)
Tplot=T(:,:,floor(0.5*M));
mesh(x(2:N-1),z(2:K-1),Tplot')
figure(3)
subplot(2,1,1)
uplot=u(:,:,floor(0.5*M));
mesh(uplot)
subplot(2,1,2)
wplot=w(:,:,floor(0.5*M));
mesh(wplot)
figure(4)
subplot(2,1,1)
plot(x,h)
subplot(2,1,2)
plot(z,hm)
figure(5)
hold on
plot(x(2:N-1),p(:,26),'r','LineWidth',2.5)
axis([min(x) max(x) -.10 .15])
xlabel('theta in rads')
ylabel('Pressure-P')
hold off
end
function [a0 a1 a2 a3 a4]=coeff1(hc,hxr,hxl,gc,gxr,gxl,hmc,hmzu,hmzd,pxr,pxl,pzu,pzd,dx,dz)
beta=1;
alpha=0.801;
a0=(2/(dx^2)+1/(2*(beta^2)*(dz^2)))*gc;
a1=((gxr-gxl)/(2*dx)).*((pxr-pxl)/(2*dx));
a2=(gc).*((pxr+pxl)/(dx^2))+((gc)/(4*beta^2)).*((pzu+pzd)/(dz^2));
a3=3*((hxr-hxl)/dx);
a4=alpha*((gc.*((hmzu-hmzd)/(2*dz)).^2)+(gc.*hmc.*((hmzu+hmzd-2*hmc)/(dz^2))));
end


function [h hm g]=coeff3(x,z)
e=0.5; v=1;L=0.2;
h=1+e*cos(x);
hm=(sin(atan(v+(2*v*z)))+sin(atan(v-(2*v*z))));
g=h.^3-12*(L^2)*h+24*(L^3)*tanh(h./(2*L));
end
function [u w]=coeff(y,hc,miuc,hmc,hmzu,hmzd,pxr,pxl,pzu,pzd,dx,dz)
Xo=0.5;
omega=0.5;
R=0.5;
Lo=1;L=0.2;
if (L>0)
u=omega*R.*(y./hc)+(0.5/miuc).*((pxr-pxl)./(2*dx)).*((y.^2-hc.*y)+(2*L^2).*(ones(size(y))-(cosh((2.*y-
hc)./(2*L)))./(eps+cosh(hc./(2*L)))));
w=(0.5/miuc).*(((pzu-pzd)./(2*dz))-Lo*Xo*hmc.*((hmzu-hmzd)./(2*dz))).*((y.^2-hc.*y)+(2*L^2).*(ones(size(y))-
(cosh((2.*y-hc)./(2*L)))./(eps+cosh(hc./(2*L)))));
else
u=omega*R.*(y./hc)+(0.5/miuc).*((pxr-pxl)./(2*dx)).*((y.^2-hc.*y));
w=(0.5/miuc).*(((pzu-pzd)./(2*dz))-Lo*Xo*hmc.*((hmzu-hmzd)./(2*dz))).*(y.^2-hc.*y);
```

```
end
end
function [T5 T6 T7 T8 T9]=temp(dx,dy,dz,miuc,Tu,Td,Tr,Tl,ur,ul,wr,wl,uc,wc)
Pr=1; Ec=1;
R=0.5;Lb=1;U=10;kmiu=0.1;
sigma=1;beta0=1;C=0.15;
T5=0.5*(((Lb^2*dz^2).*(Tr+Tl))+((R^2*dx^2).*(Tu+Td)))./(((Lb^2)*dz^2)+(R^2*dx^2));
T6=0.25*Pr*(U/kmiu)*((R*Lb*dx*dz)/((Lb^2*dz^2)+(R^2*dx^2)))*((Lb*dz*uc.*(Tr-Tl))+(R*dx*wc.*(Tu-Td)));
T7=((R^2*Lb^2*dx^2*dz^2)/((Lb^2*dz^2)+(R^2*dx^2)));
T8=Ec*(Pr/C^2)*(0.5/max(dy))*(0.5/max(dy))*miuc*((ur-ul).^2+(wr-wl).^2);
T9=Ec*Pr*0.5*((sigma*(beta0^2))/kmiu)*(uc.^2+wc.^2);
end
```

APPENDIX 2: PUBLICATION